

NATIONAL ADVISORY COMMITTEE FOR AERONAUTICS

WARTIME REPORT

ORIGINALLY ISSUED
January 1943 as
Memorandum Report

FULL-SCALE TUNNEL TESTS OF A FLYING MODEL OF THE
CURTISS XP-55 AIRPLANE

By William J. Biebel

Langley Memorial Aeronautical Laboratory
Langley Field, Va.

CASE FILE
COPY

JPL LIBRARY
CALIFORNIA INSTITUTE OF TECHNOLOGY

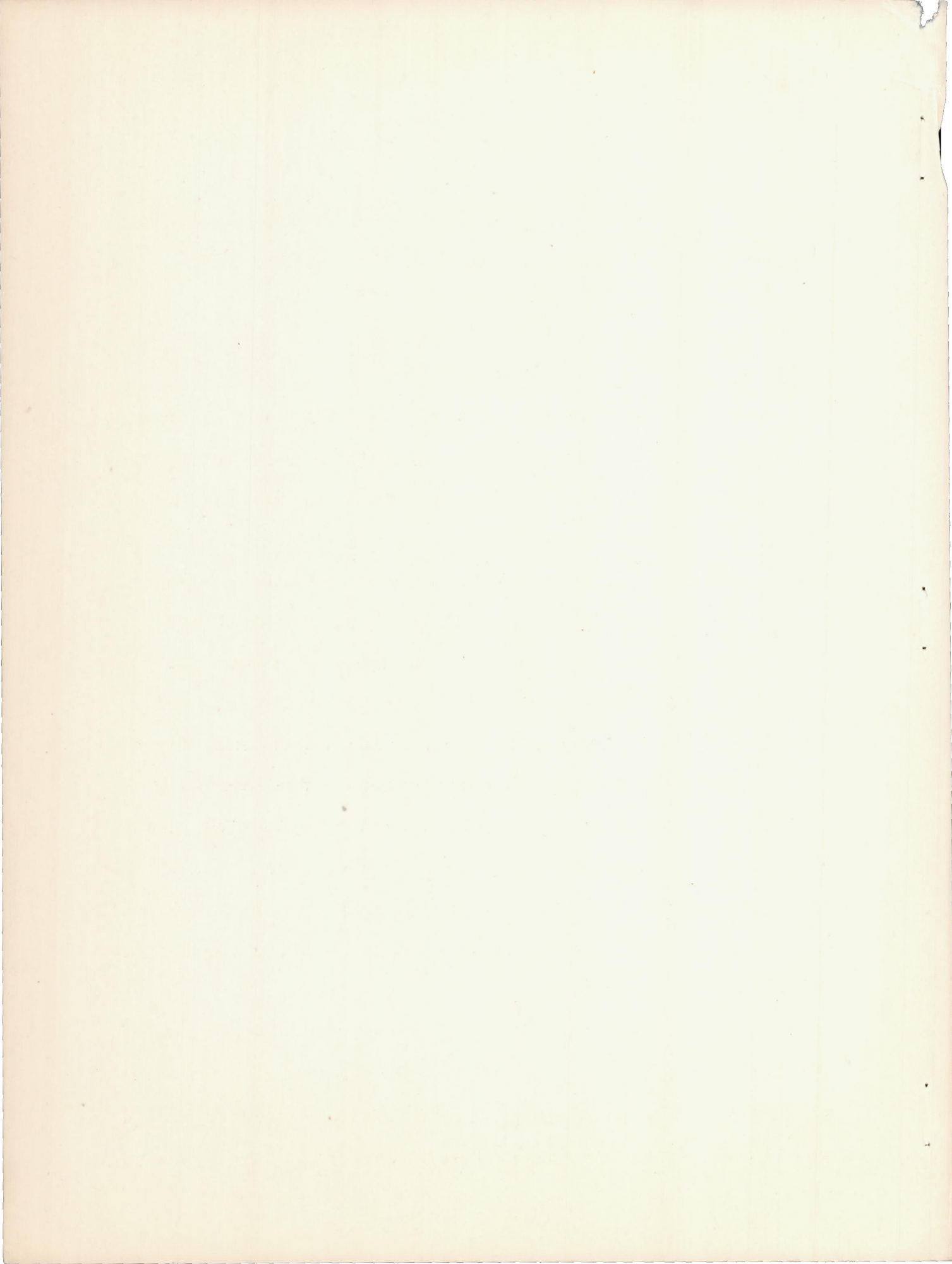


WASHINGTON

MAR 1 - 1948

NACA WARTIME REPORTS are reprints of papers originally issued to provide rapid distribution of advance research results to an authorized group requiring them for the war effort. They were previously held under a security status but are now unclassified. Some of these reports were not technically edited. All have been reproduced without change in order to expedite general distribution.

L-627



MEMORANDUM REPORT

for

Army Air Forces, Materiel Command

FULL-SCALE TUNNEL TESTS OF A FLYING MODEL OF THE
CURTISS XP-55 AIRPLANE

By William J. Biebel

INTRODUCTION

At the request of the Army Air Forces, Materiel Command, tests have been conducted in the NACA full-scale tunnel to provide data for estimating the longitudinal stability and control characteristics of the Curtiss XP-55 airplane. The XP-55 is a low-wing airplane with the engine and propeller located at the rear of the fuselage. Longitudinal and directional control are obtained by means of a "nose" elevator and by fins and rudders attached near the wing tips.

The tests included lift, drag, pitching-moment, hinge-moment, and elevator pressure measurements for various combinations of angle of attack, elevator deflection, and elevator tab settings. The stalling characteristics of the wing were investigated by tuft surveys. The drag increments due to the gun blast tubes and the external elevator balance units were also measured.

The results of the force tests and some correlation of the results of the force tests and the pressure measurements are presented in this report. The complete results of the pressure-distribution tests will be presented in a subsequent report.

SYMBOLS

- C_L lift coefficient
- C_D drag coefficient
- C_m pitching-moment coefficient about the center of gravity
- C_{H_e} elevator hinge-moment coefficient $\left(\frac{H_e}{q_o S_e \bar{c}_e}\right)$
- H_e elevator hinge moment, positive when moment tends to move trailing edge downward
- q dynamic pressure $\left(\frac{1}{2}\rho v^2\right)$
- V velocity
- ρ density
- S wing area
- S_e elevator area (excluding fuselage)
- \bar{c}_e root-mean-square elevator chord
- α angle of attack of thrust line relative to free-stream direction
- δ_e elevator deflection relative to thrust axis, positive with trailing edge down
- δ_{eT} elevator tab deflection relative to elevator chord line, positive with trailing edge down

Subscripts:

- t horizontal tail
- o free stream
- T tab

APPARATUS AND TESTS

The tests were conducted on the Curtiss C-24B airplane (figs. 1 and 2) which is a light-weight, low-powered flying model of the XP-55 airplane. Prior to the tests, modifications were made to the C-24B airplane so that it would more closely represent the XP-55 airplane. These modifications included: (1) installation of a nose elevator similar to that of the XP-55 airplane, (2) removal of the landing gear, and (3) resurfacing of the wing so as to obtain a smooth finish. The airplane is arranged as a low-wing pusher with an engine installed in the rear of the fuselage. The wing sections are similar to NACA low-drag airfoil sections and the wing has a sweepback angle of 28.5° and a dihedral angle of 4.5° .

Longitudinal control is obtained by means of an all-movable surface located at the nose of the fuselage. The nose elevator was fitted with orifices for the pressure measurements. The elevator is equipped with trim tabs having a span of 50 percent of the elevator span and a mean chord of 25 percent of the mean elevator chord. The elevator was directly connected to the stick, but the tab angle was adjusted by means of a separate control in the cockpit.

All the tests were made with the propeller removed. The tests to investigate the longitudinal stability of the model included measurements of the forces and moments on the model at various angles of attack with the elevator removed

and attached. The effects of elevator and elevator tab deflections on pitching moments and hinge moments were investigated through a range of angles of attack of the thrust axis from about -2° to 16° . These tests included the determination of the effects of deflecting the flaps 45° . The elevator hinge moments were determined from measurements of the forces on the stick at various elevator and elevator tab deflections. Figure 3 shows the relationship between stick force and hinge moment for the various elevator deflections. The range of elevator and elevator tab deflections for the above tests was from -30° to 20° .

Drag tests were made with the gun blast tubes sealed and unsealed (fig. 4) and with the external elevator balance units attached (fig. 5) and removed (fig. 6). The effect of fairing the hatch gun blast tubes (fig. 7) was investigated.

The stalling characteristics of the wing were studied by tuft surveys and force tests. Motion pictures were made of the tufts to supplement the visual observations.

One scale-effect test was made at speeds from about 63 to 85 miles per hour. All other tests were made at a tunnel airspeed of about 63 miles per hour corresponding to a Reynolds number of about 3,200,000 based on the mean aerodynamic chord (5.47 feet).

RESULTS AND DISCUSSION

Longitudinal Stability and Control

Force tests. - The airplane pitching moments were calculated about a center of gravity located at 12 percent of the mean aerodynamic chord (fig. 2). The variation of pitching-moment coefficient with angle of attack of the airplane with the elevator removed and with the elevator fixed at various angular deflections for the flaps-retracted condition is shown in figure 8. Similar curves are given in figure 9 for the airplane with wing flaps deflected 45° . The slope of the pitching-moment curve against angle of attack was negative with the elevator removed and was positive with the elevator installed for all the elevator angles up to 10° . With the elevator deflected 10° , the slope was negative for angles of attack above 4° and with the elevator deflected 20° , the slope was negative for all angles of attack. At $\delta_e = 20^\circ$ the elevator was stalled for all angles of attack. Flap deflection resulted in increasing the slope of the curve of the pitching-moment coefficient against angle of attack in the direction to improve the stability.

The elevator angles (measured relative to the thrust axis) required for trim with the stick fixed and with the tab neutral are plotted against angle of attack in figures

10 and 11. The slope of the curve of $d\delta_e/d\alpha$ is considerably less with the flaps deflected 45° than with the flaps retracted.

The data show that the airplane, in the propeller-removed condition, is longitudinally unstable with the elevator fixed. With the stick free, however, the stability is adequate, as will be discussed later, and the stick forces are applied in the same direction as for a conventional, stable airplane. The stick-fixed instability will be decreased in power-on flight as a result of the stabilizing effect of the propeller forces. These results are essentially in agreement with observations made on a 1/10-scale model in the NACA free-flight tunnel.

The pitching moments due to the elevator have been determined for various angles of attack and elevator deflections, by comparing the results of the tests with the elevator attached and removed, and are shown in figures 12 and 13. For the range of elevator angles tested, the slopes of the curves of tail pitching-moment coefficient against angle of attack are essentially the same for all elevator angles up to 10° . At an elevator deflection of 10° the slope of the curve of tail pitching-moment coefficient against angle of attack decreased at high angles of attack, and at 20° elevator deflection the slope was lower at all angles of attack. A comparison has been made in figures 14 and 15 of the tail

pitching-moment coefficients determined from the force tests and the values obtained from the pressure measurements. The agreement is satisfactory except at the high angles of attack where the pitching moments obtained from the pressure measurements were appreciably lower than those obtained from the force tests.

The variations of the airplane pitching-moment coefficient with elevator deflection for various angles of attack are shown in figure 16 with the flaps retracted and in figure 17 with the flaps deflected 45° . The slope $dC_m/d\delta_e$ remained essentially constant in both cases for all angles of attack at elevator deflections below the stall. Flap deflection produced only a negligible change in the elevator effectiveness. The value of $dC_m/d\delta_e$ determined from the tests was about 0.0090 per degree elevator deflection.

The effects of tab deflection at various elevator angles on the pitching-moment coefficients of the model with the flaps retracted are shown in figures 18 and 19 for angles of attack of -0.6° and 10.5° , respectively. At an angle of attack of -0.6° the tab effectiveness changed only slightly for the different elevator angles. At an angle of attack of 10.5° the tab effectiveness remained essentially constant up to an elevator angle of 5° and decreased at elevator angles higher than 5° .

Elevator hinge moments and stick forces. - Figures 20 and 21 show the variation of elevator hinge-moment coefficient with angle of attack at various elevator angles for the airplane with flaps retracted and with flaps deflected 45° . The variations of elevator hinge-moment coefficient with elevator deflection at various angles of attack have been determined by cross-plotting the results of figures 20 and 21 and are given in figures 22 and 23. The elevator hinge moments were determined from stick-force measurements. The value of $dC_{h_e}/d\alpha$ increased slightly with elevator deflection and the value of $dC_{h_e}/d\delta_e$ increased slightly with angle of attack. At zero elevator deflection, the slope $dC_{h_e}/d\alpha$ was about -0.0043 per degree and at zero angle of attack the slope $dC_{h_e}/d\delta_e$ was about -0.0042 per degree. Flap deflection had little effect on the slopes $dC_{h_e}/d\alpha$ and $dC_{h_e}/d\delta_e$.

Values for the elevator "floating angles" determined from the elevator hinge-moment measurements are given in figures 24 and 25 for various angles of attack. It is seen that the change of elevator free-floating angle for a given change in angle of attack is greater than unity. Studies of the pressure distribution over the elevator surfaces indicate that when the elevator angle is equal but of opposite sign to the angle of attack there exists an upload on the rear of the elevator adjacent to the fuselage. Since the center

of pressure of this load is in back of the elevator hinge line, the elevator, when free, floats nose down with respect to the wind direction at positive angles of attack.

The variations of pitching-moment coefficient with angle of attack with the elevator freely floating are shown in figure 26 for flaps retracted and in figure 27 for flaps deflected 45° . These curves were determined from pitching-moment measurements at zero elevator hinge-moment coefficient. Figure 26 indicates that with the elevator freely floating and with the flaps retracted, the airplane will be longitudinally stable at angles of attack below 11.2° ($C_L = 0.36$) and unstable at higher angles of attack. With flaps deflected 45° (fig. 27) the slope of the pitching-moment curve indicates positive stability at angles of attack below 10.2° and neutral stability at higher angles of attack. Because of the tendency of the elevator to float nose down with respect to the wind direction, the slope of the pitching-moment curve against angle of attack is slightly more negative with the elevator free than with the elevator removed. The slope of the moment curve dC_m/da was -0.0053 at $C_m = 0$ with flaps retracted and was -0.0106 with the flaps deflected 45° .

Curves of elevator hinge-moment coefficient against angle of attack have been plotted for the trim condition with stick fixed by determining the hinge moments corresponding to the elevator angles for trim at various angles

of attack (zero tab deflection) and are shown in figures 28 and 29. Examination of the data reveals that the direction of the forces on the stick is similar to the direction of the stick forces on a conventional, stable airplane. Flap deflection increased the slope of the curve of elevator hinge-moment coefficient against elevator deflection for the stick-fixed trim condition.

The effect of tab deflection on elevator hinge moments for various angular deflections of the elevator is shown in figure 30 for an angle of attack of -0.6° . The variation of $dC_{h_e}/d\delta_{e_T}$ with elevator deflection was small for the range of elevator angles tested. The value of $dC_{h_e}/d\delta_{e_T}$ was about -0.0085 at zero elevator hinge moment.

Drag of Gun Blast Tubes and Elevator Balance Units

The effects of the gun blast tubes on the airplane lift and drag coefficients are shown in figure 31. The minimum drag coefficient of the airplane with all the gun blast tubes sealed was 0.0214 . No appreciable change of minimum drag coefficient was measured when the blast tubes were unsealed or when a fairing was installed over the hatch gun blast tubes.

Since external mass balancing on the elevator of the XP-55 airplane is contemplated, tests were made to determine the effect of the balance units on minimum drag. The results of these tests are shown in figure 32. The increment of minimum drag coefficient due to the addition of the two

external elevator balance units shown in figure 4 was 0.0007. This result appears to be higher than would be expected for this type of balance installation.

Aerodynamic Characteristics of the Airplane

The variations of lift, drag, and pitching-moment coefficients with angle of attack for the airplane with the elevator removed and attached are shown in figure 33 with flaps retracted and in figure 34 with flaps deflected 45° . The maximum lift coefficient of the untrimmed model with the flaps retracted was 1.075, which increased to 1.20 when the flaps were deflected 45° . The stall occurred at an angle of attack of 16° with flaps retracted and at 14° with flaps deflected 45° .

Tuft observations of the stall characteristics of the wing are shown in figures 35 to 38 at four angles of attack ($\alpha = 8.5^\circ, 13.2^\circ, 15.1^\circ, \text{ and } 17.3^\circ$) with flaps retracted. For the four angles of attack the flow at the trailing edge of the wing was outboard toward the wing tips and parallel to the trailing edge of the wing. The flow at the wing-fuselage juncture was steady until the stall of the entire wing occurred. Wing stall occurred first at the wing tips at an angle of attack of 15.1° and progressed inboard with increasing angle of attack such that at an angle of attack of 17.3° the wing was almost completely stalled.

Scale Effect on Lift and Drag

The effect of Reynolds number on the lift and the drag of the airplane is shown in figure 39. There was no appreciable change in lift coefficient for the range of Reynolds numbers tested; the drag decreased, however, with increasing Reynolds number. At a Reynolds number of 4,320,000 the minimum drag coefficient was 0.0208 compared with a value of 0.0216 at a Reynolds number of 3,220,000.

SUMMARY OF RESULTS

1. The XP-55 airplane was longitudinally unstable in the propeller-removed condition with the stick fixed. With the stick free and the landing flaps retracted, the airplane was longitudinally stable at angles of attack below 11.2° and unstable at higher angles of attack.
2. Deflecting the flaps 45° decreased the instability with stick fixed and increased the stability with stick free.
3. The elevator effectiveness changed very little with angle of attack or flap deflection. A value of $dC_m/d\delta_e$ of about 0.0090 was measured.
4. The rate of change of elevator hinge-moment coefficient with elevator deflection at zero angle of attack was about -0.0042 per degree and the rate of change of elevator hinge-moment coefficient with angle of attack at zero elevator deflection was about -0.0048 per degree.

5. The change of elevator "free-floating" angle for a given change of angle of attack was greater than unity; namely, the elevator floated nose down with respect to the wind direction at positive angles of attack.

6. The rate of change of elevator hinge-moment coefficient per degree change in elevator tab angle was about -0.0035 .

7. The increment of minimum drag coefficient due to the gun blast tubes was small.

Langley Memorial Aeronautical Laboratory,
National Advisory Committee for Aeronautics,
Langley Field, Va., January 29, 1943.

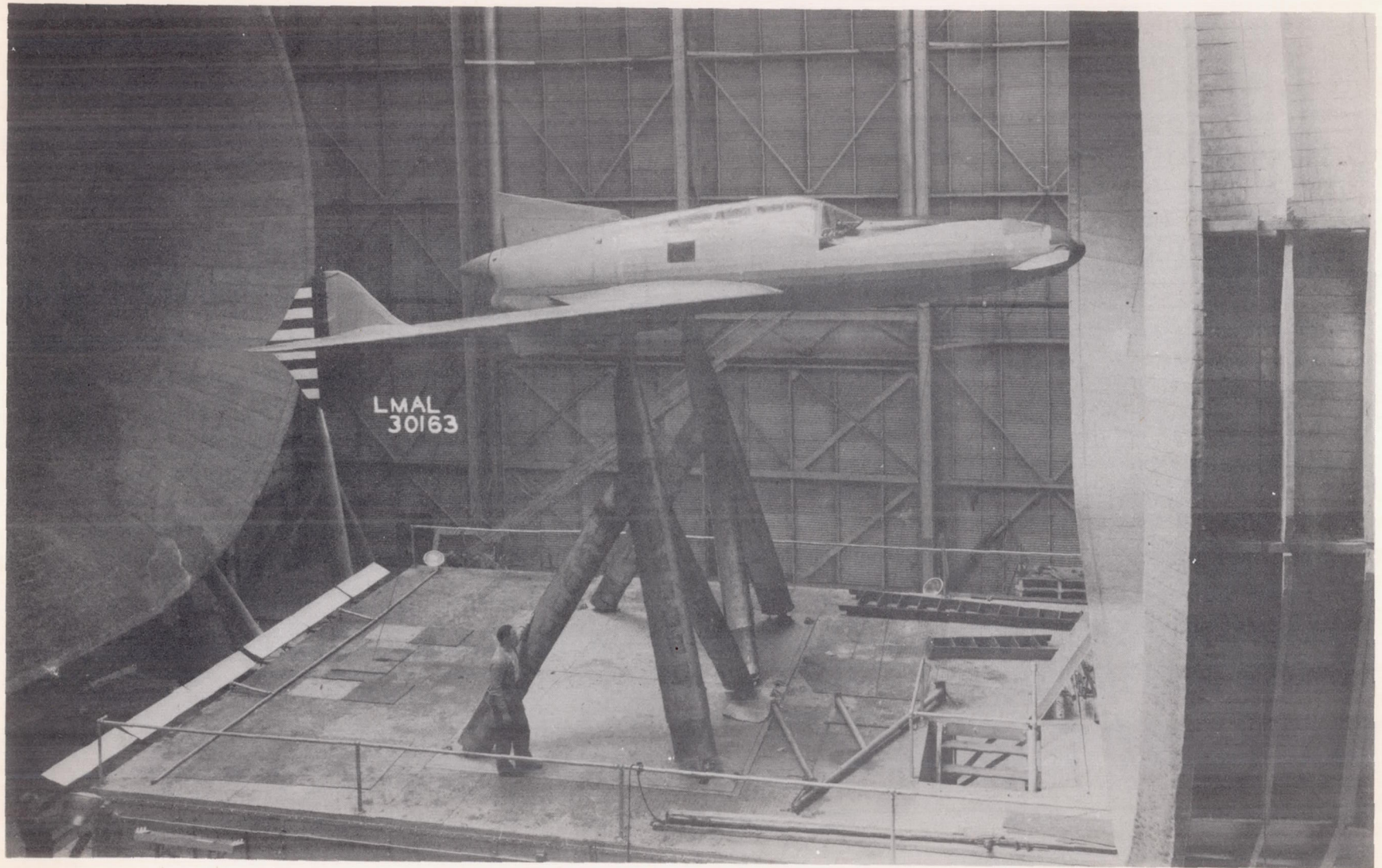


Figure 1.- The flying model of the XP-55 airplane mounted in the full-scale tunnel.

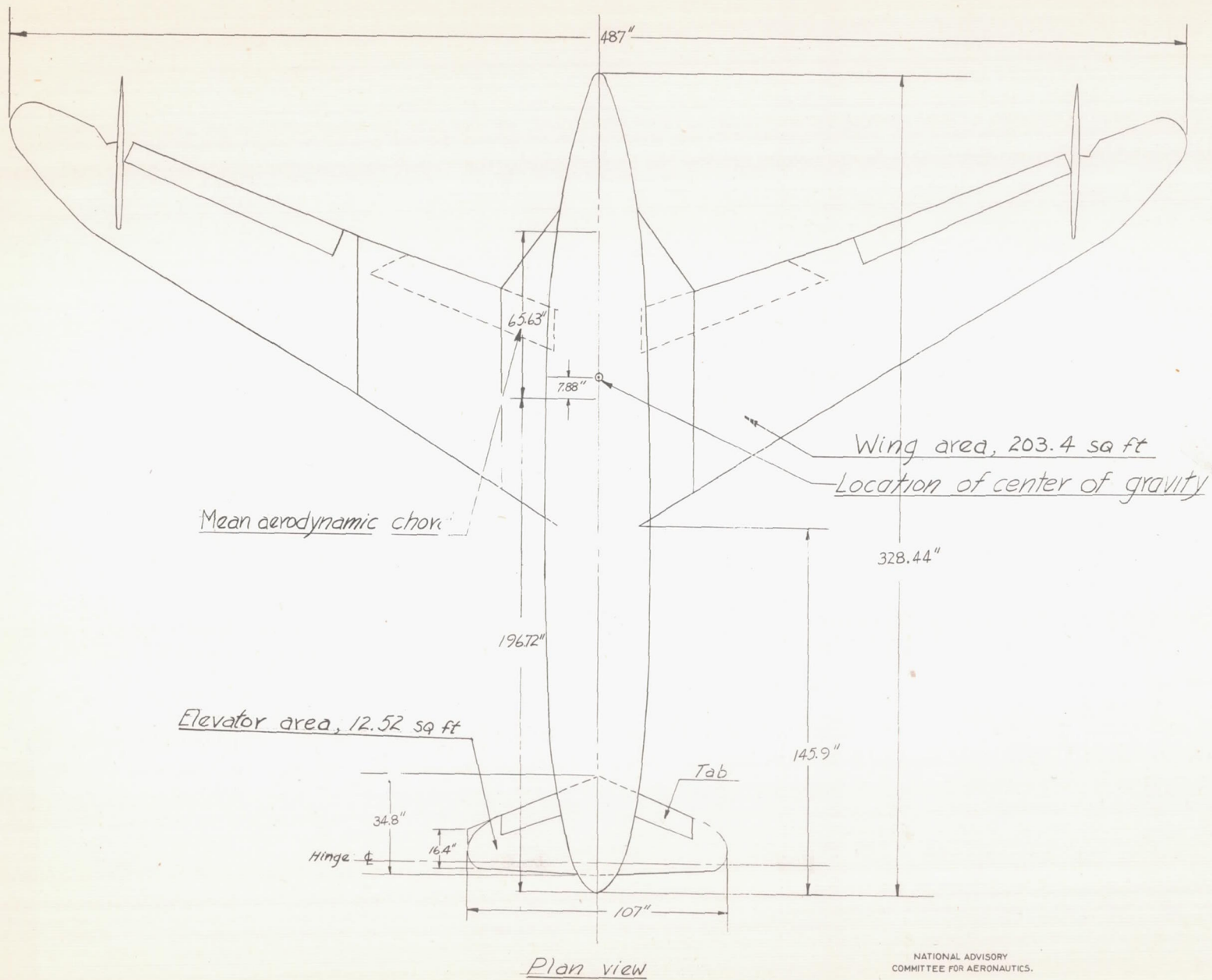


Figure 2.- Flying model of the XP-55 airplane.

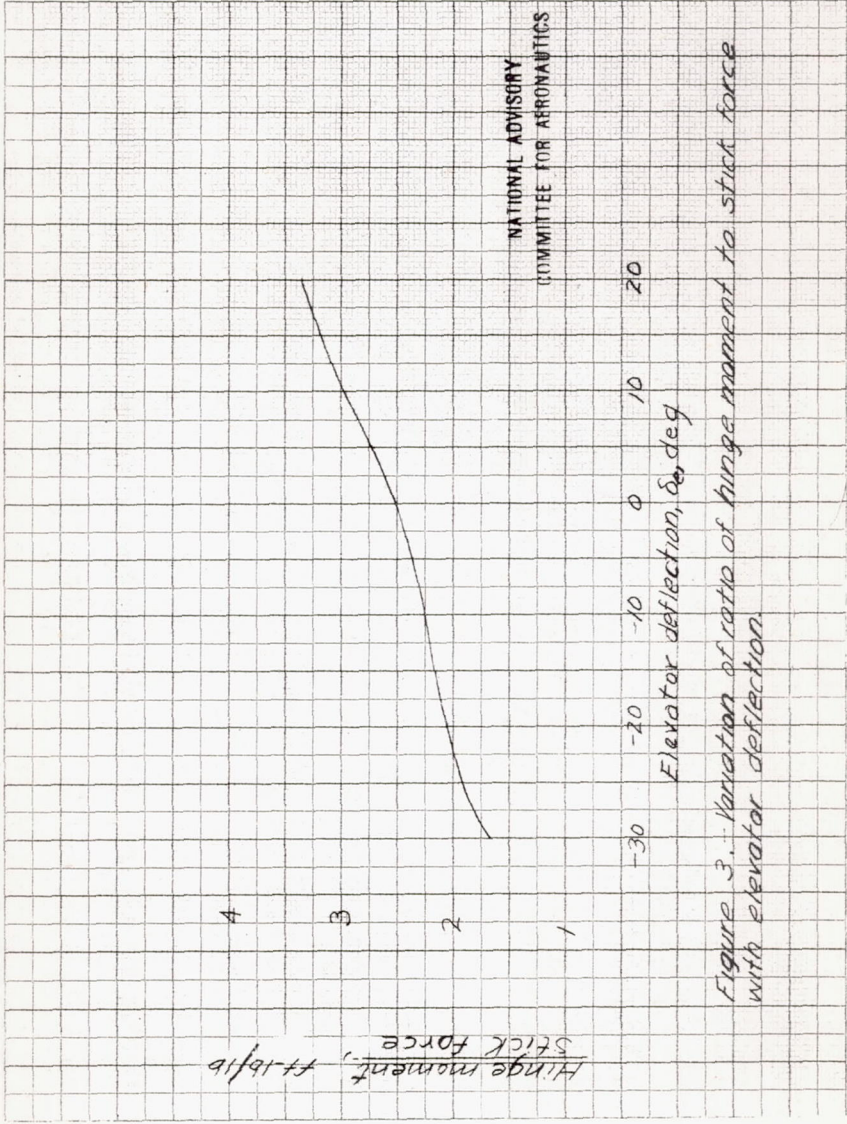


Figure 3. Variation of ratio of hinge moment to stick force with elevator deflection.

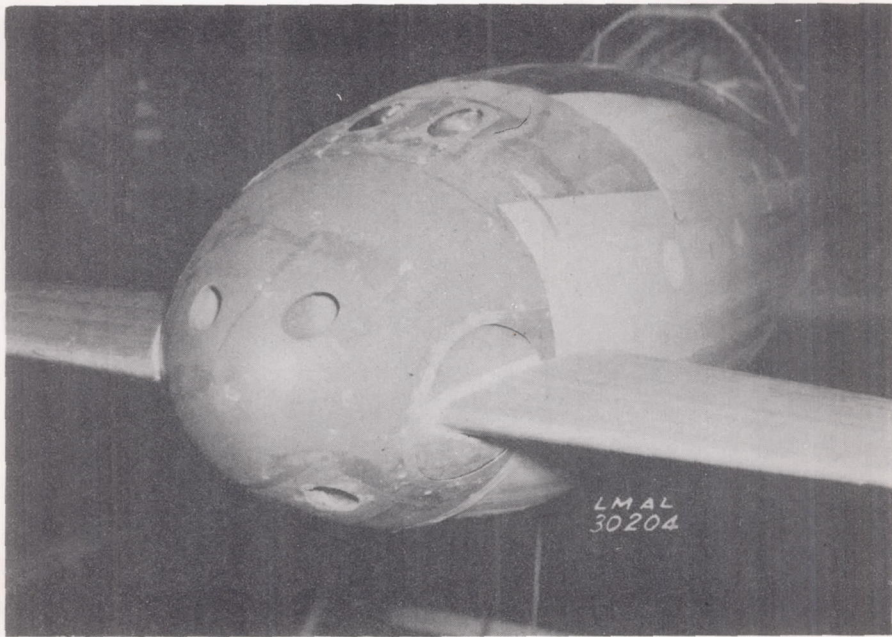


Figure 4.- The nose of the XP-55 model showing the gun blast tubes unsealed.

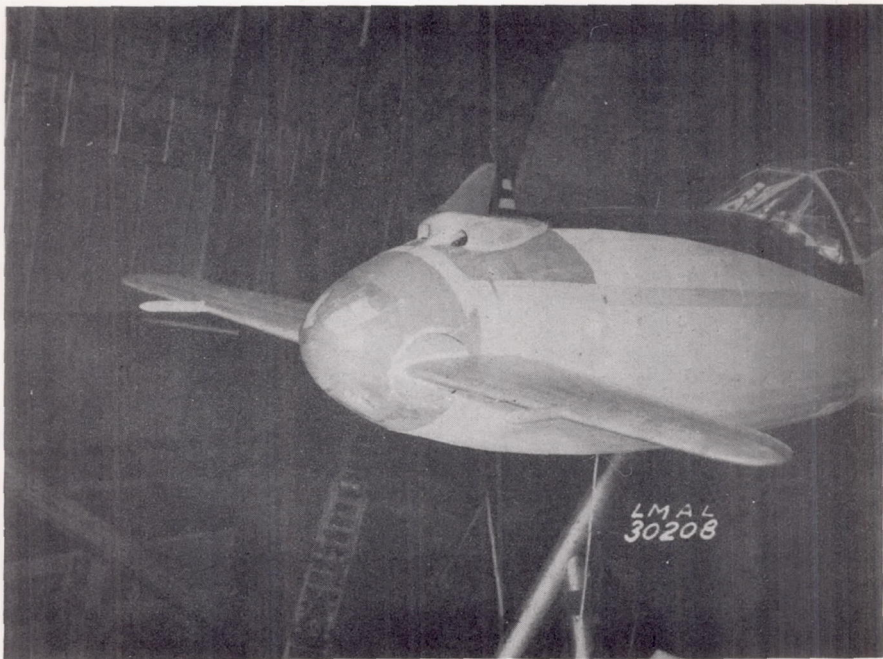


Figure 5.- The balance units attached to the XP-55 elevator

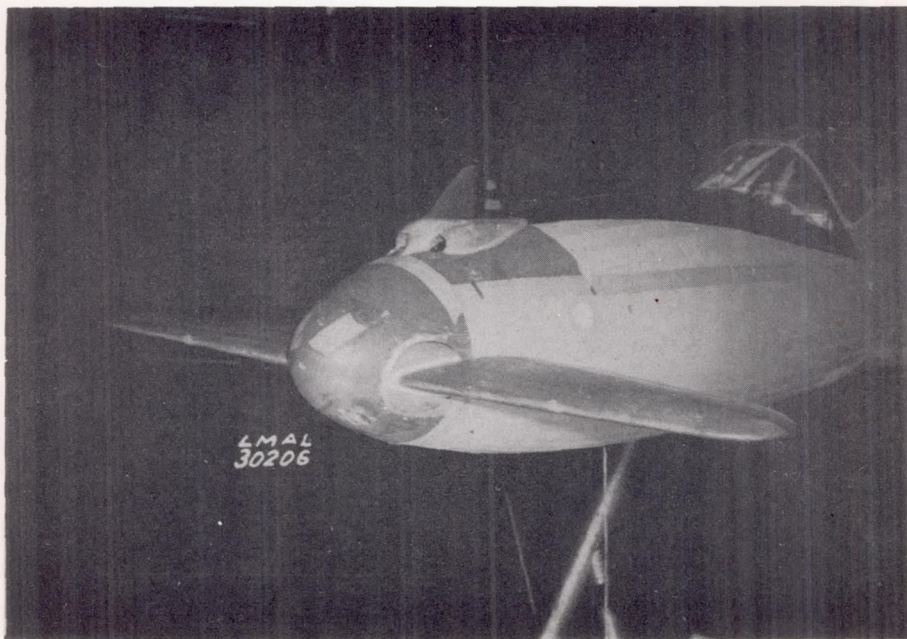


Figure 6.- The XP-55 elevator with balance units removed.

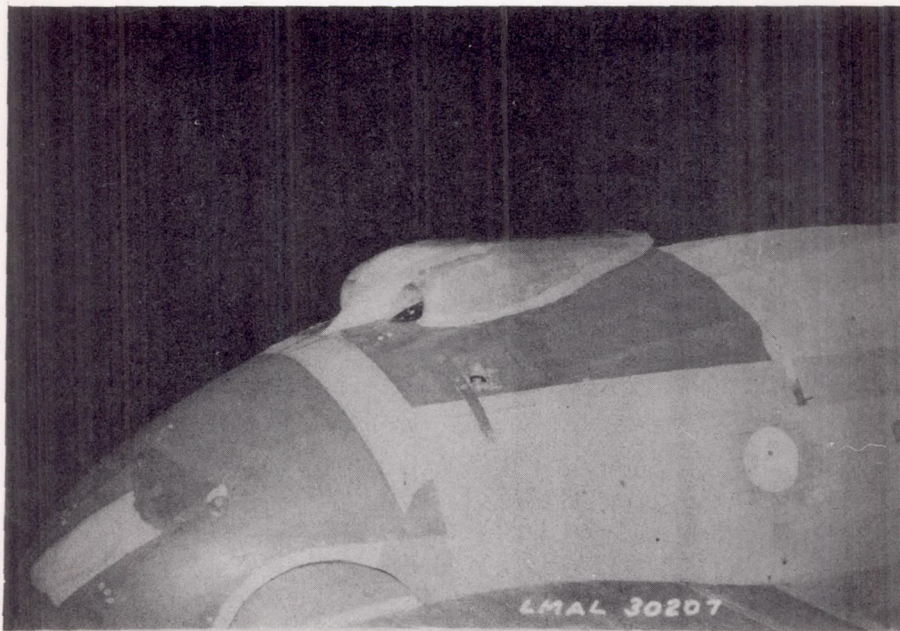


Figure 7.- The hatch gun blast tubes in the faired condition.

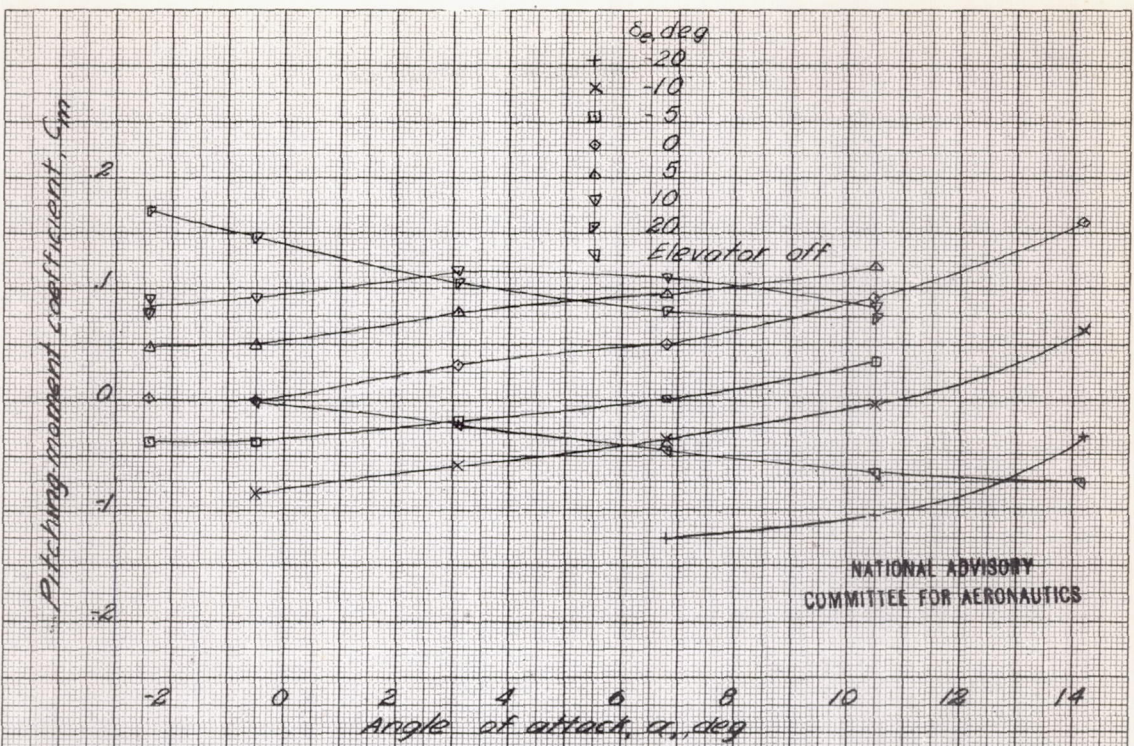


Figure 8-Variation of pitching-moment coefficient with angle of attack. Tab neutral; flaps retracted.

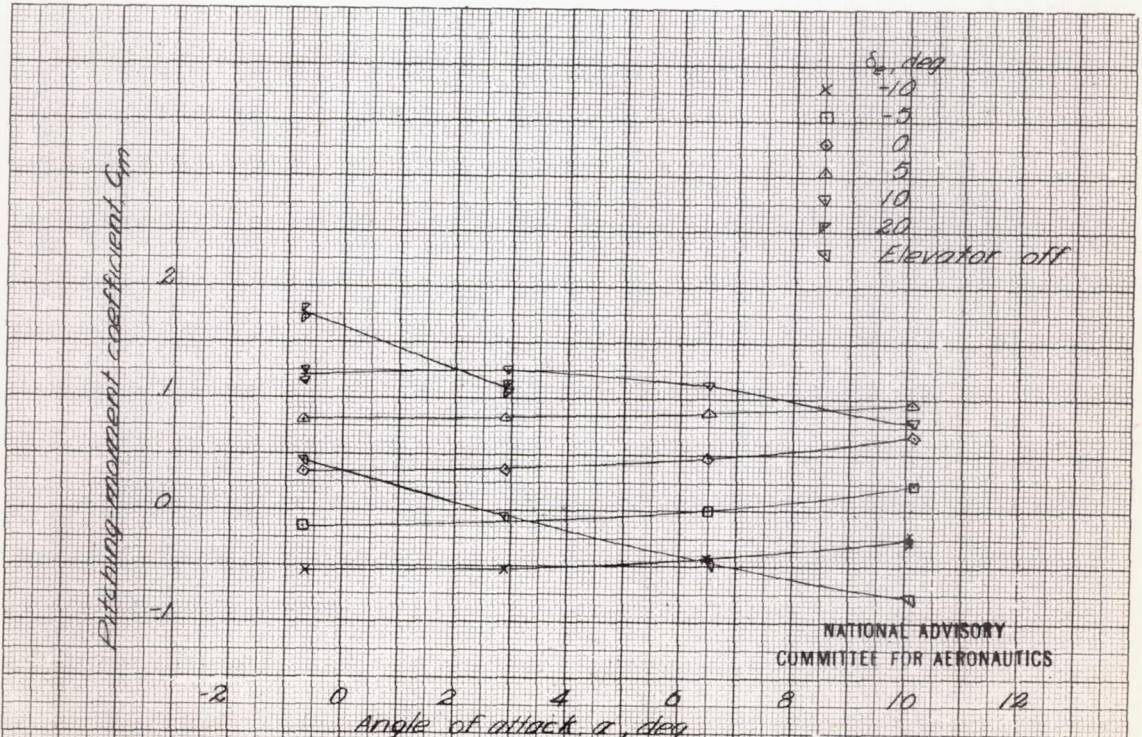


Figure 9-Variation of pitching-moment coefficient with angle of attack. Tab neutral; flaps deflected 45°.

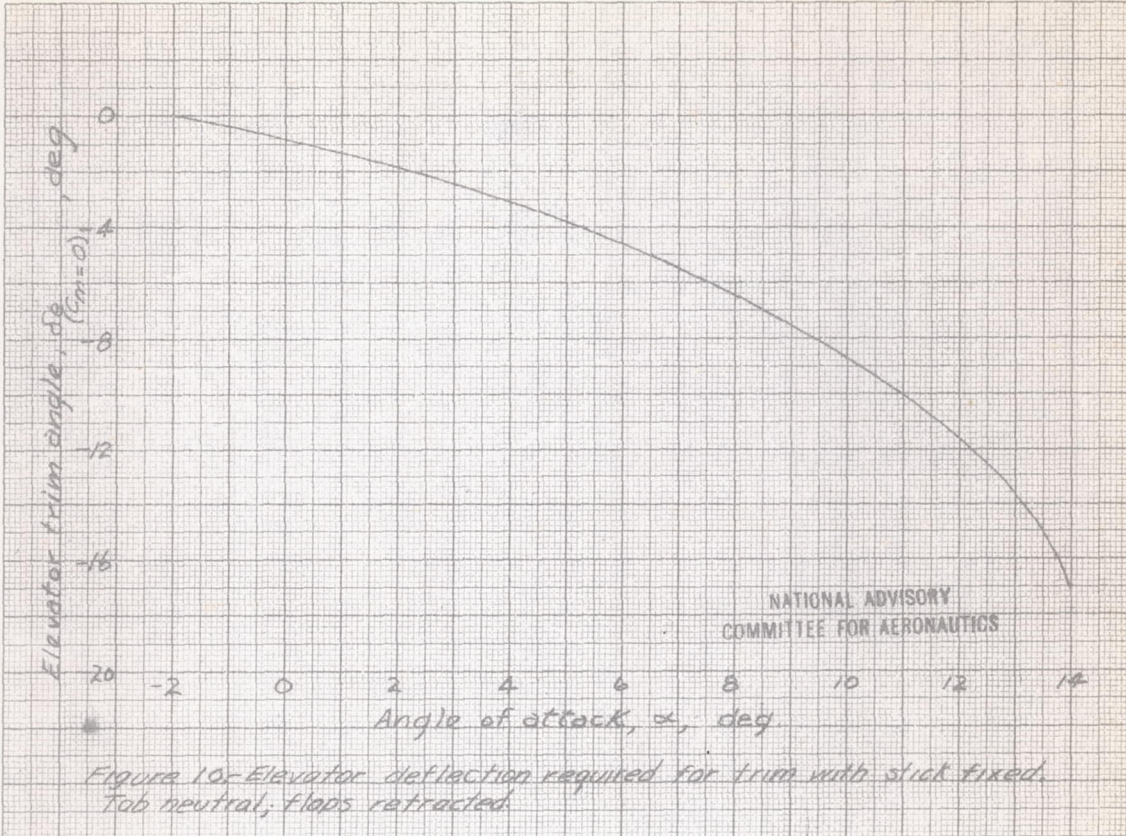


Figure 10 - Elevator deflection required for trim with stick fixed, Tab neutral, flaps retracted.

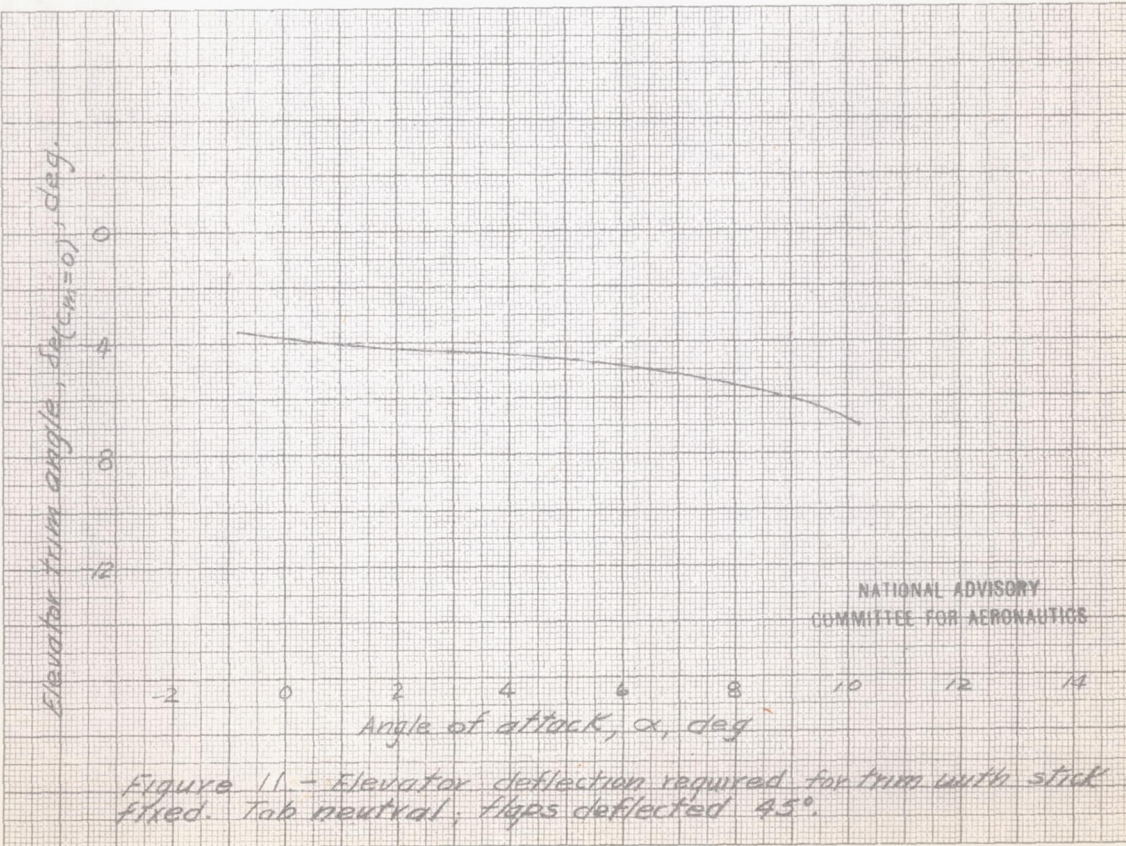


Figure 11 - Elevator deflection required for trim with stick fixed, Tab neutral, flaps deflected 45°.

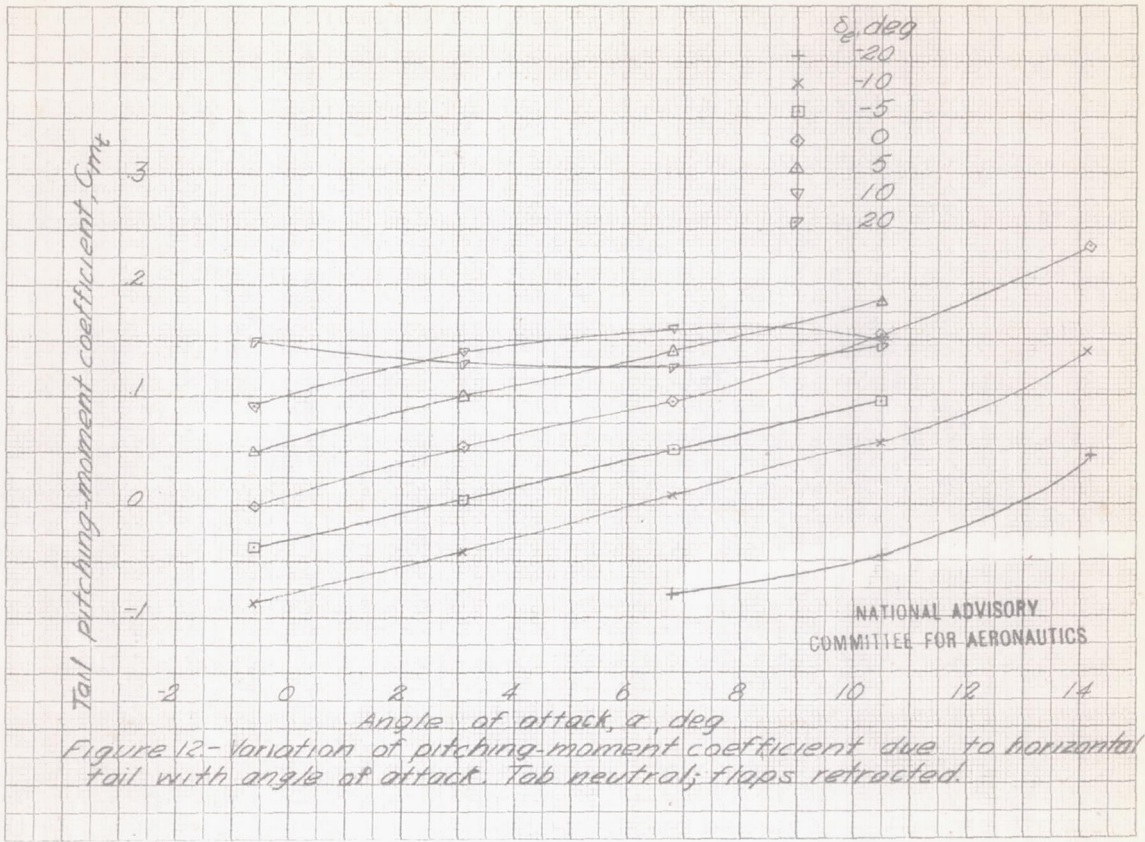


Figure 12-Variation of pitching-moment coefficient due to horizontal tail with angle of attack. Tab neutral; flaps retracted.

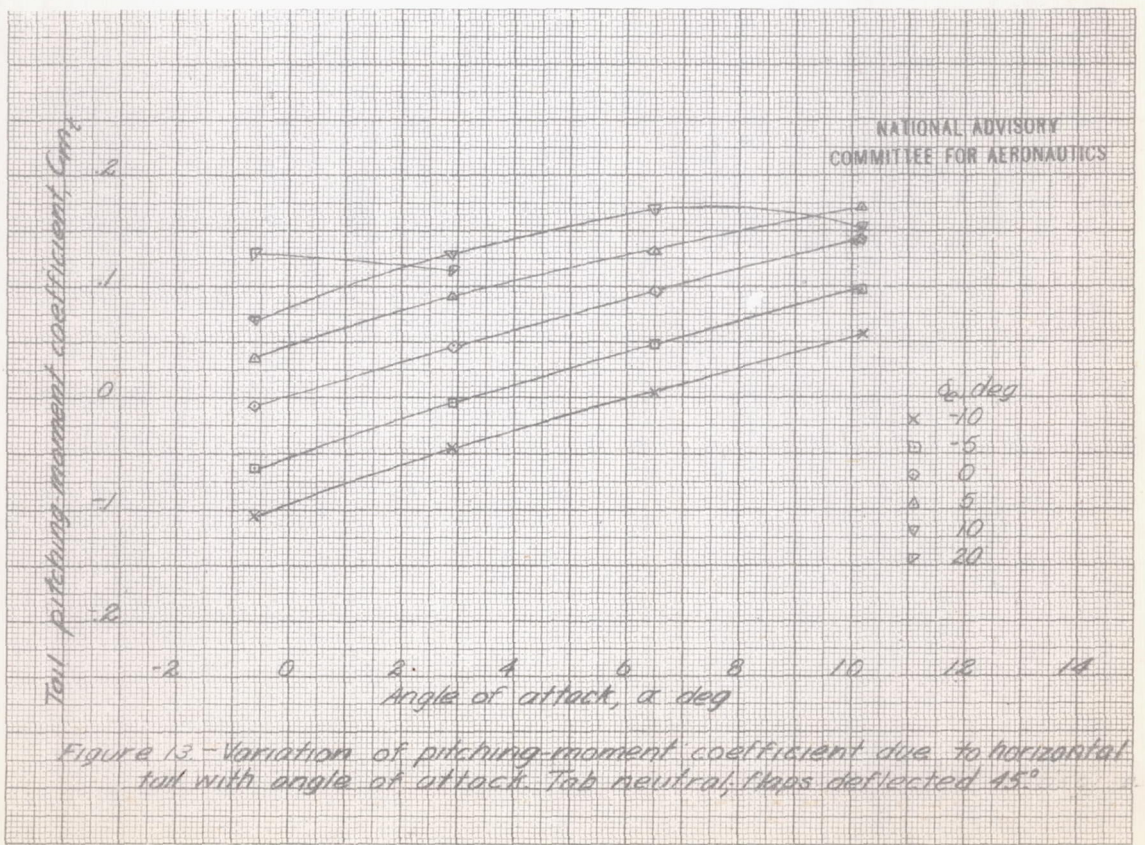


Figure 13-Variation of pitching-moment coefficient due to horizontal tail with angle of attack. Tab neutral; flaps deflected 45°.

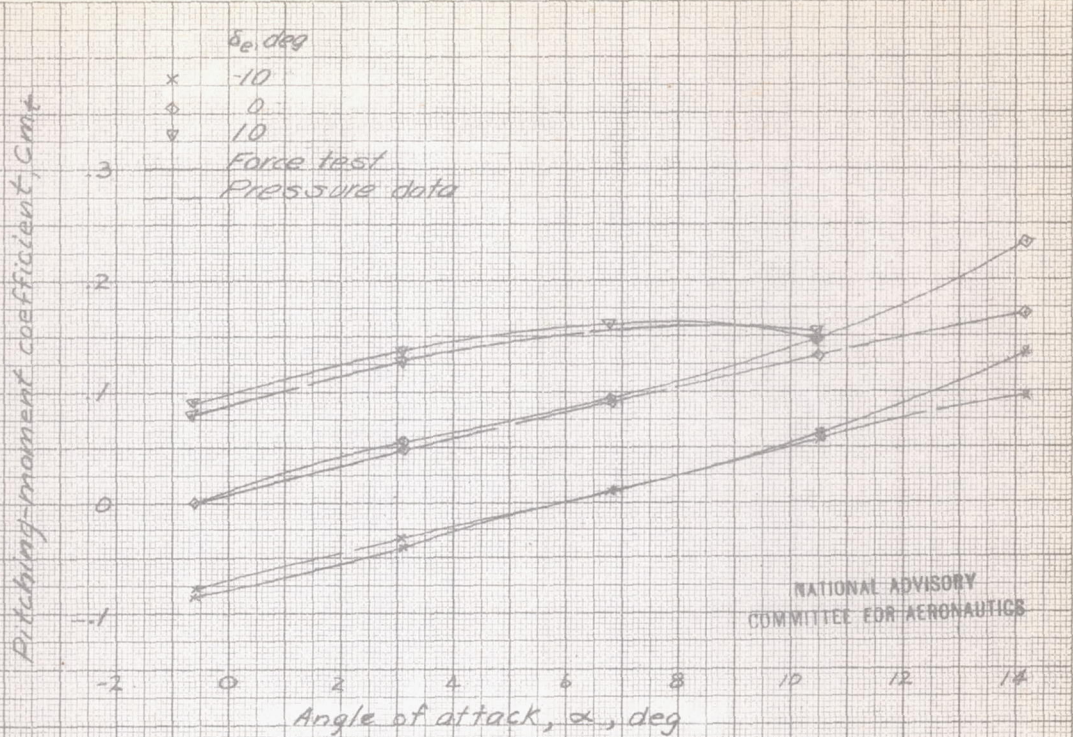


Figure 14.- Variation of pitching-moment coefficient due to horizontal tail with angle of attack, calculated from force tests and pressure data. Tab neutral, flaps retracted.

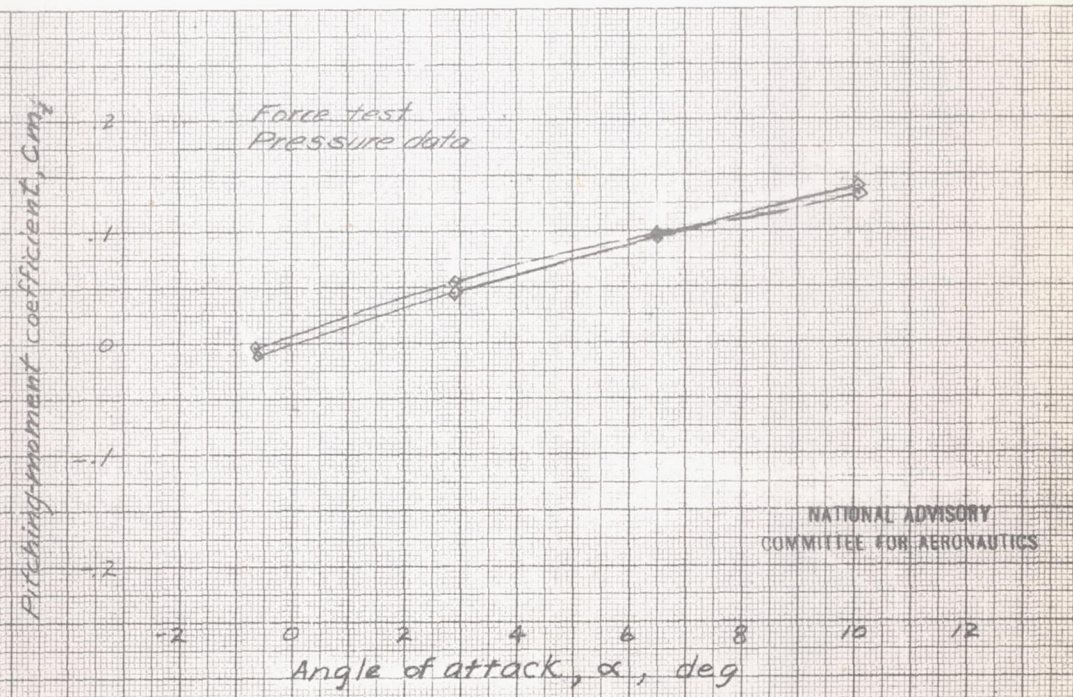


Figure 15.- Variation of pitching-moment coefficient due to horizontal tail with angle of attack, calculated from force tests and pressure data. Elevator and tab neutral. Flaps deflected 45°.

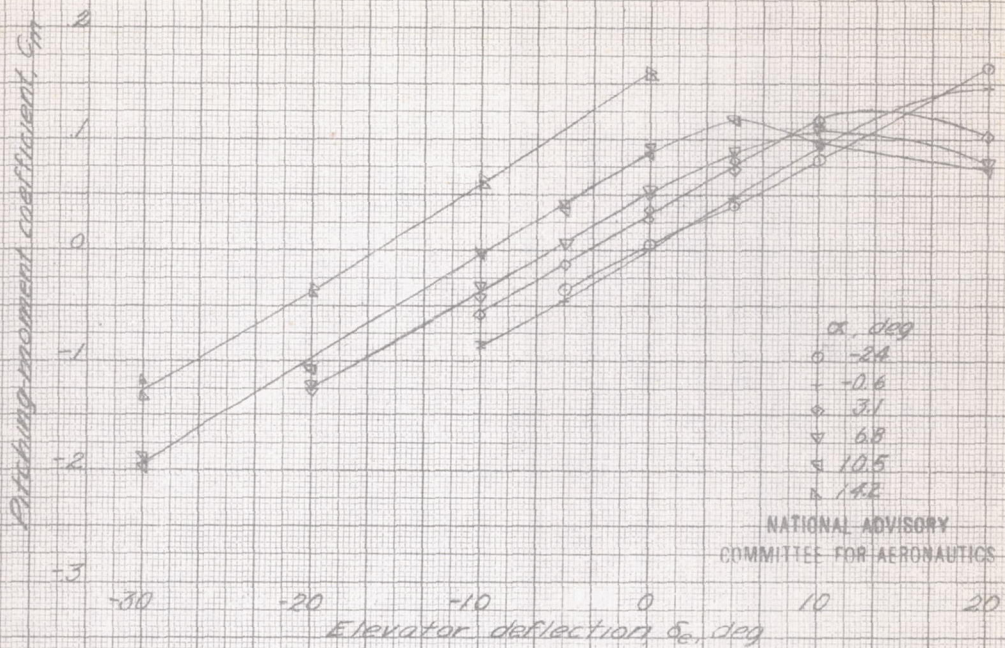


Figure 16.- Variation of pitching-moment coefficient with elevator deflection at various angles of attack. Tab neutral; flaps retracted.

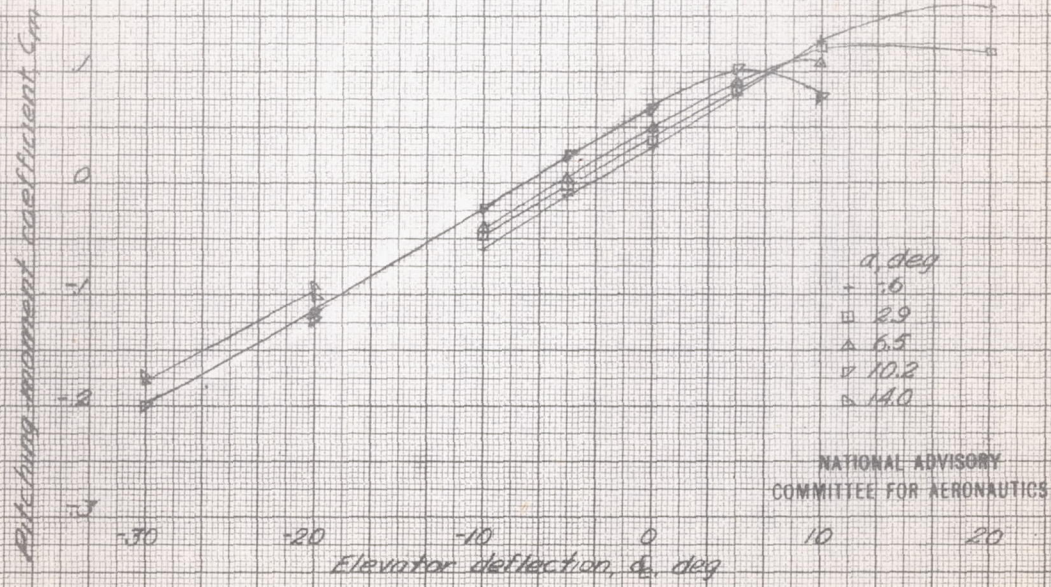


Figure 17.- Variation of pitching-moment coefficient with elevator deflection at various angles of attack. Tab neutral; flaps deflected 45°.

NATIONAL ADVISORY
COMMITTEE FOR AERONAUTICS

NATIONAL ADVISORY
COMMITTEE FOR AERONAUTICS

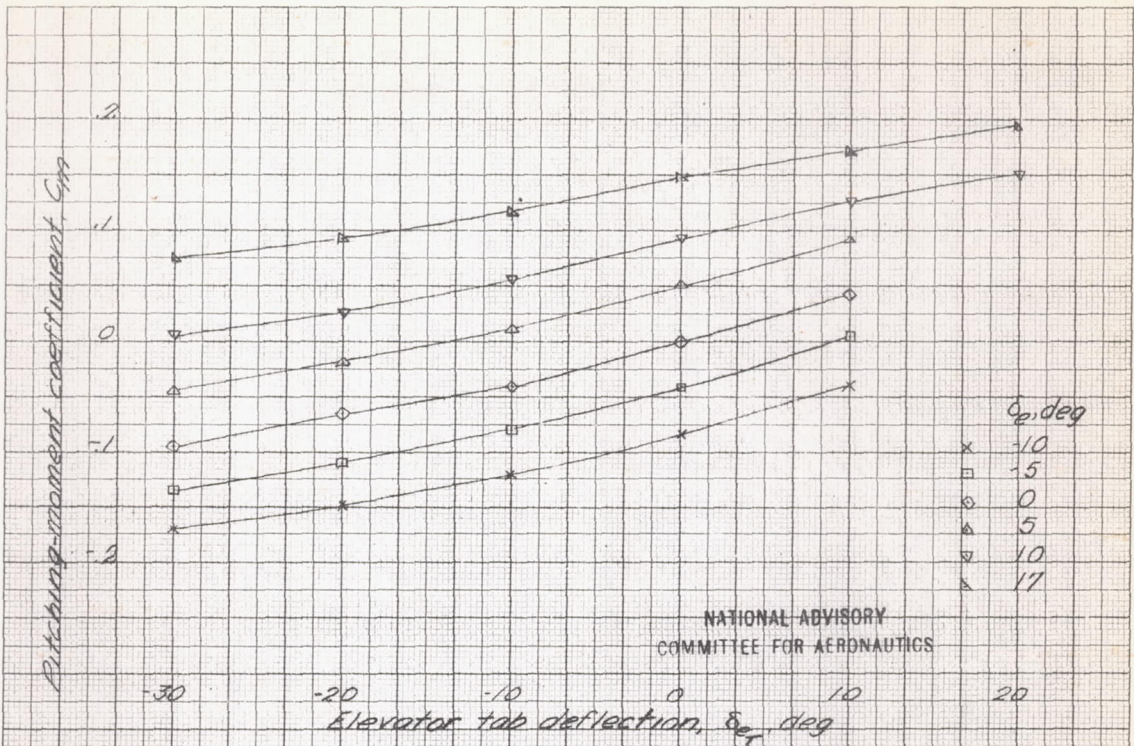


Figure 18.- Variation of pitching-moment coefficient with elevator tab deflection at various elevator deflections $\alpha, -0.6^\circ$; flaps retracted.

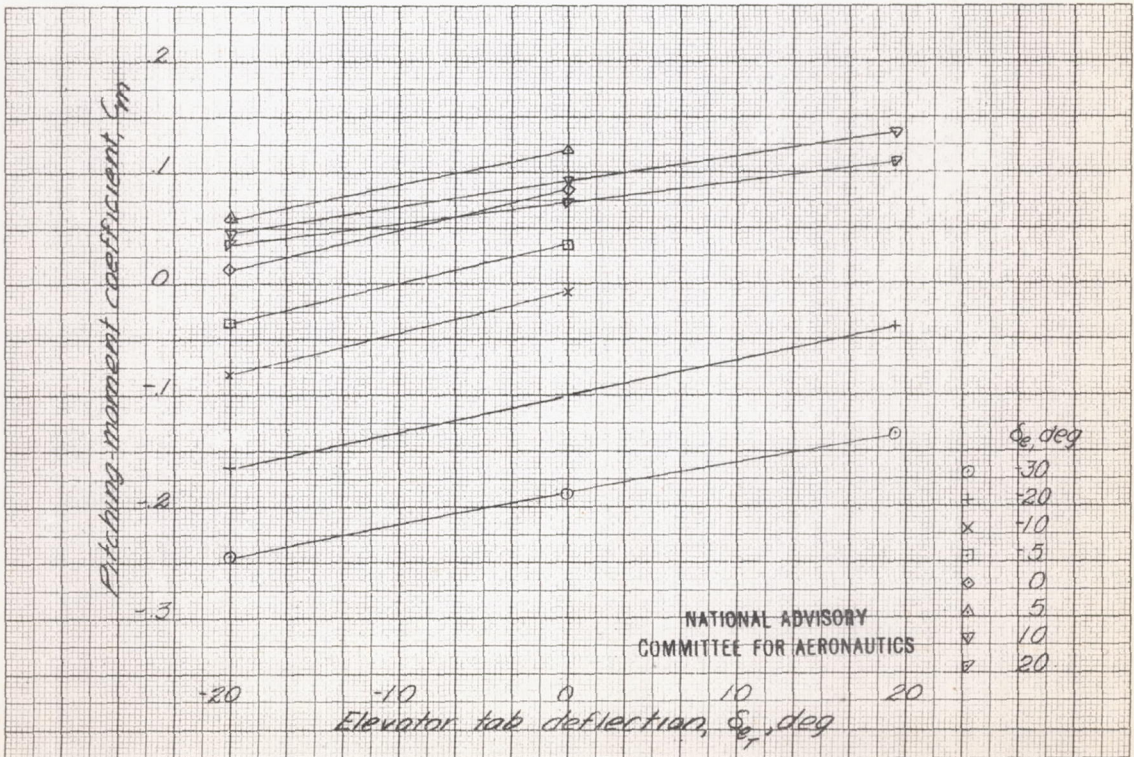
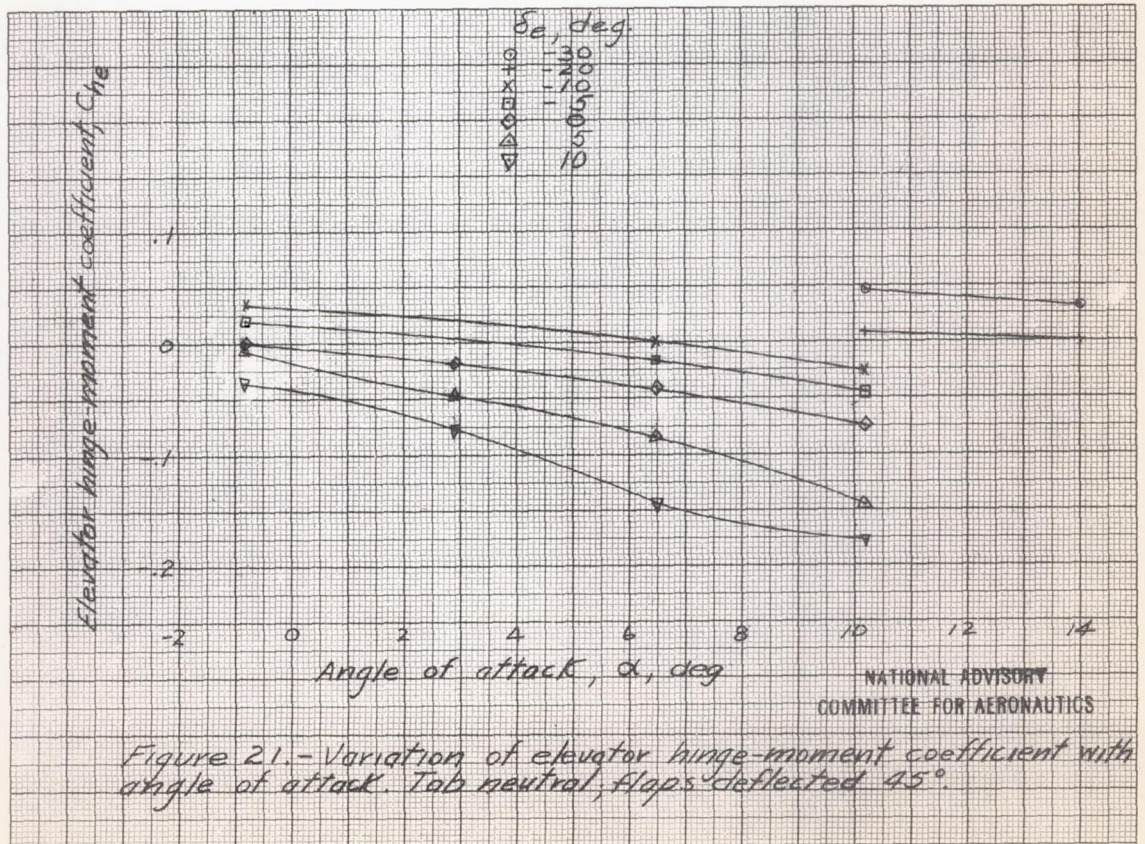
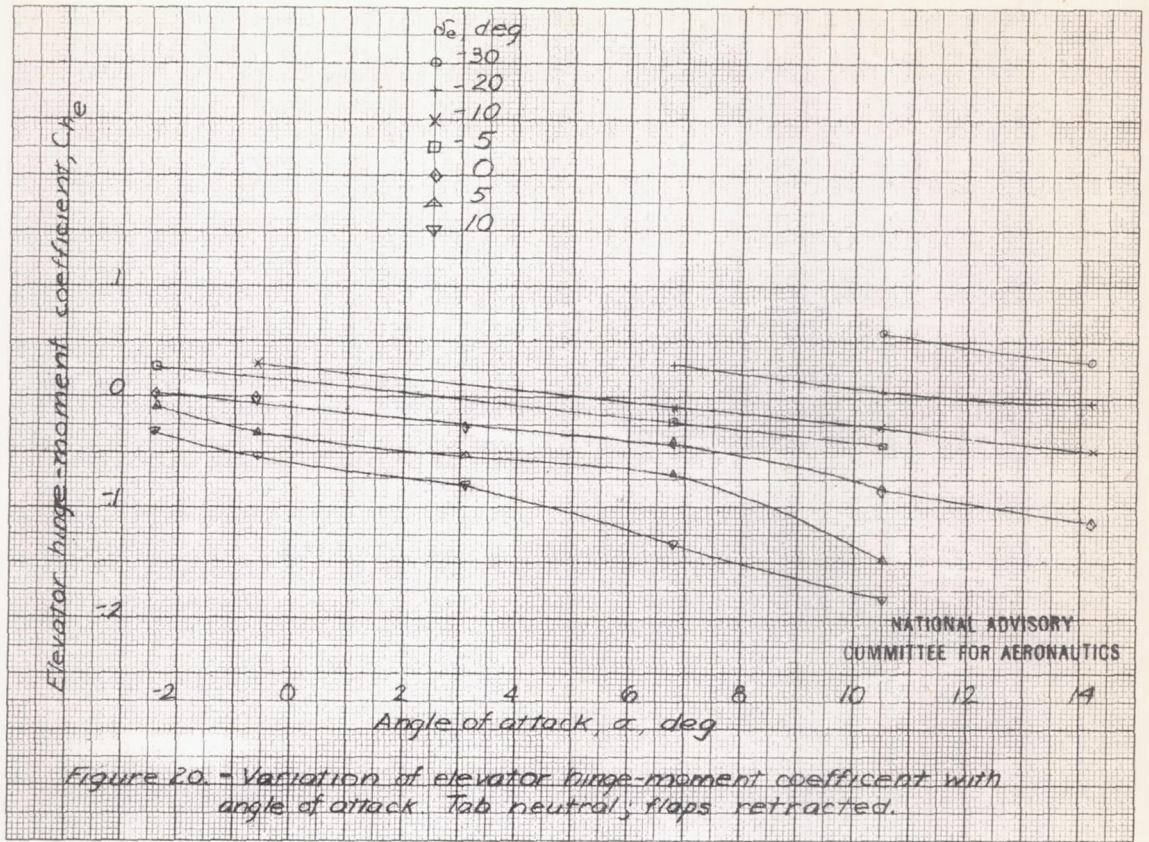


Figure 19.- Variation of pitching-moment coefficient with elevator tab deflection at various elevator deflections $\alpha, 10.5^\circ$; flaps retracted.



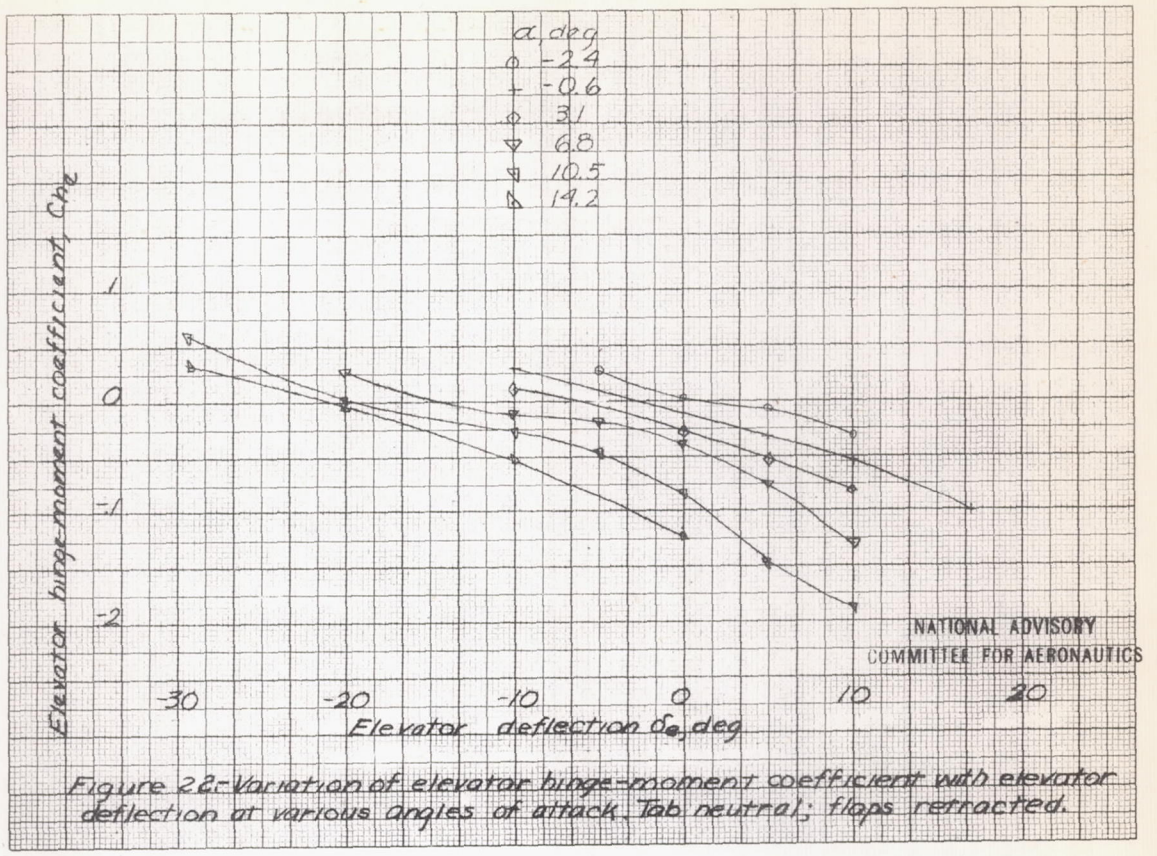


Figure 22.- Variation of elevator hinge-moment coefficient with elevator deflection at various angles of attack. Tab neutral; flaps retracted.

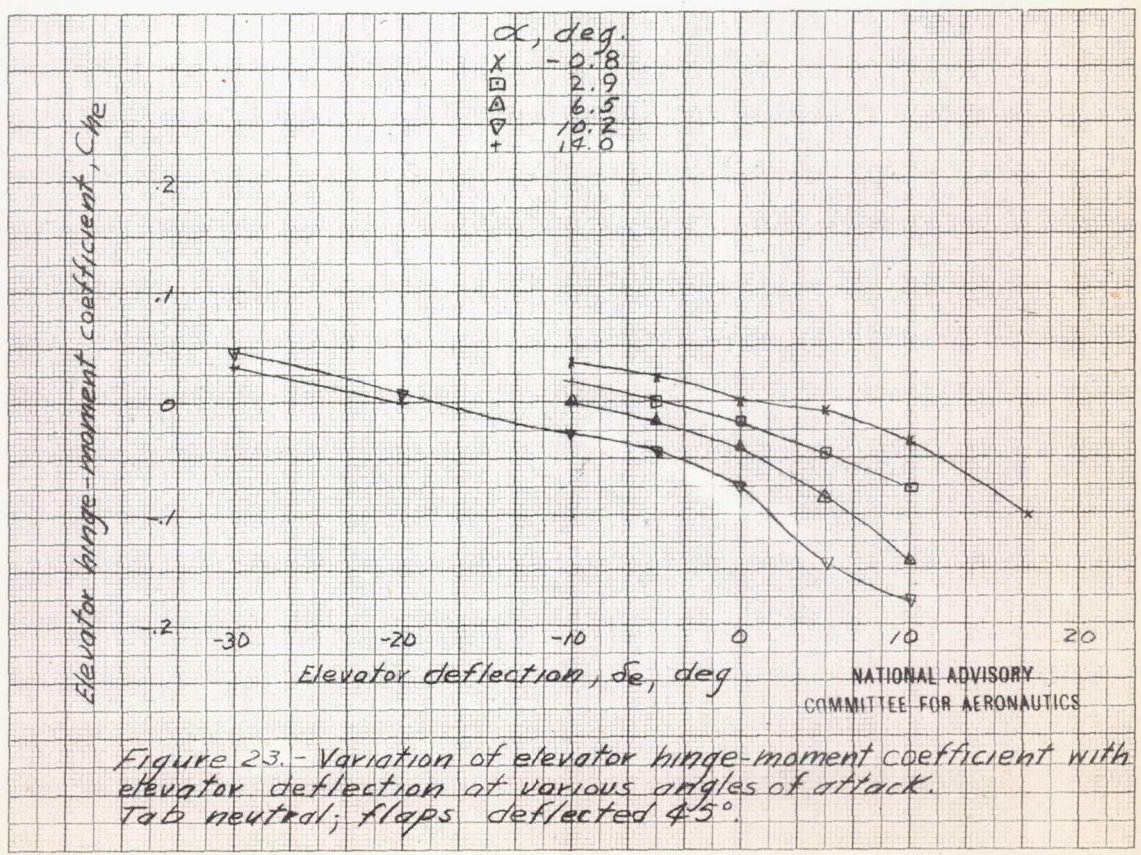
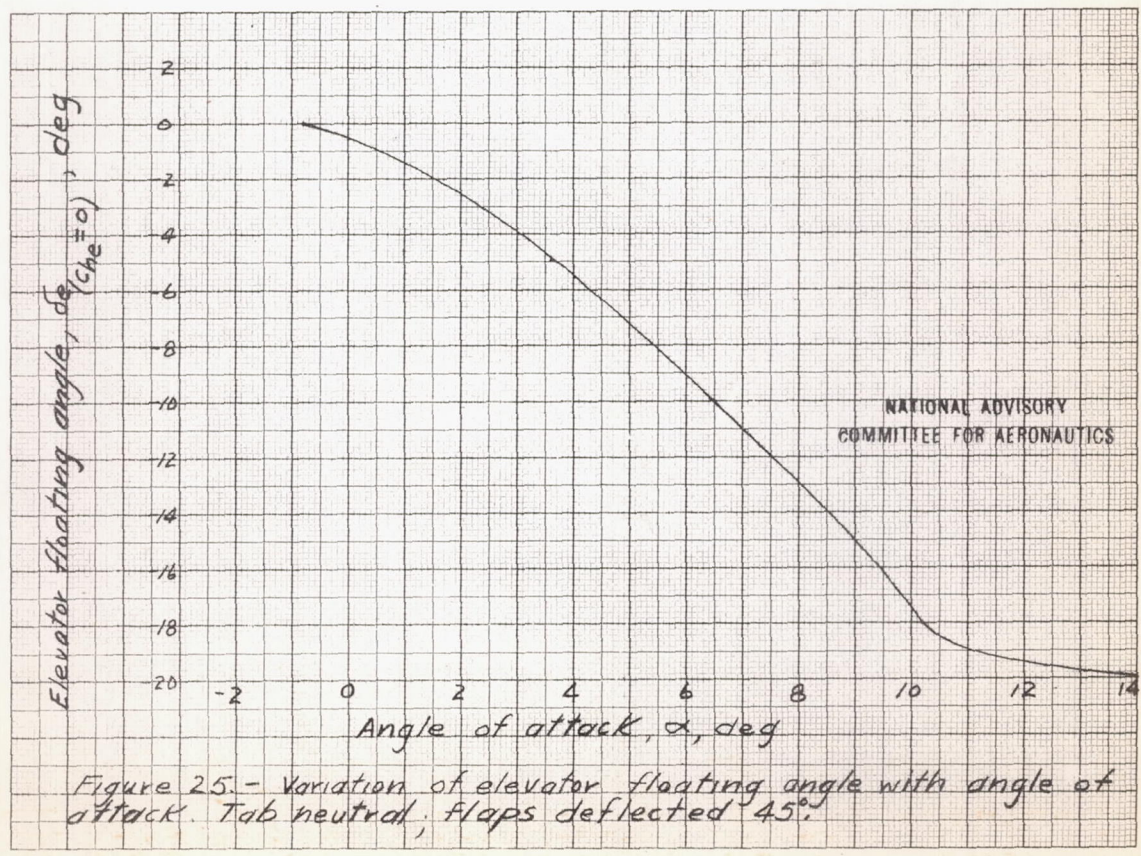
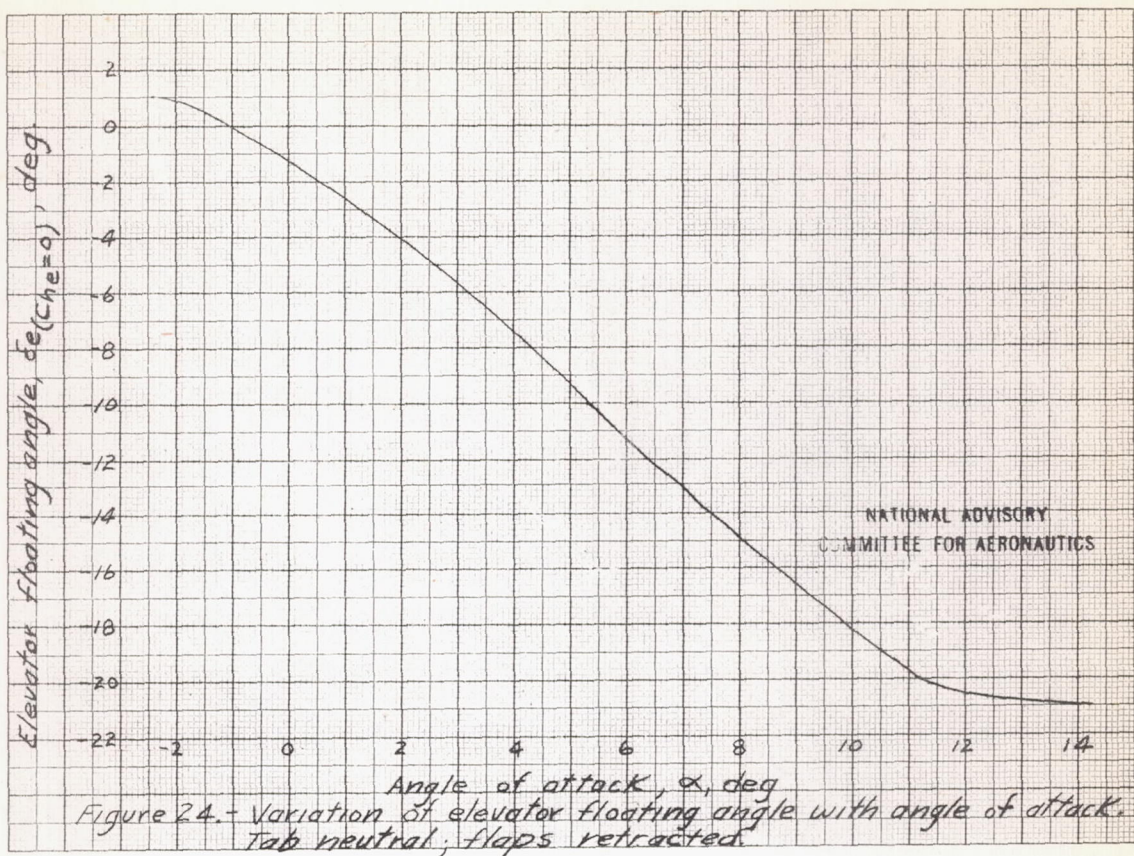
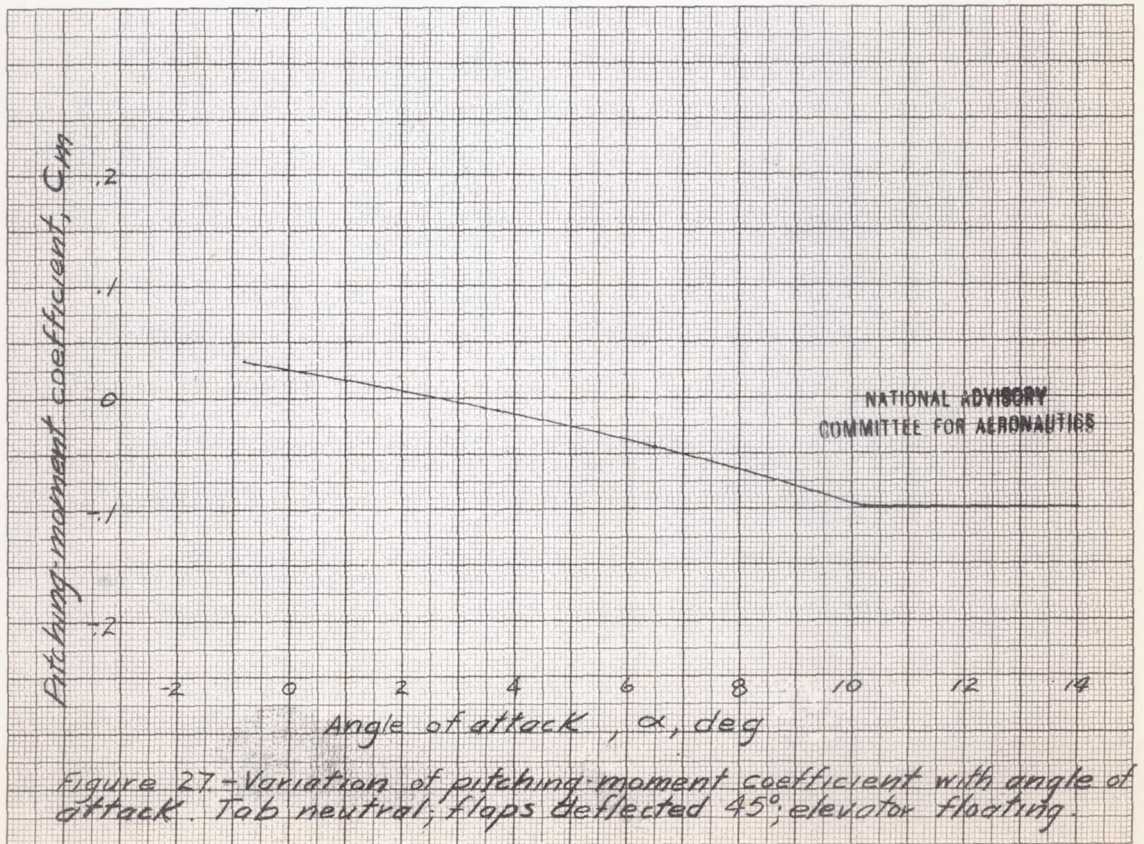
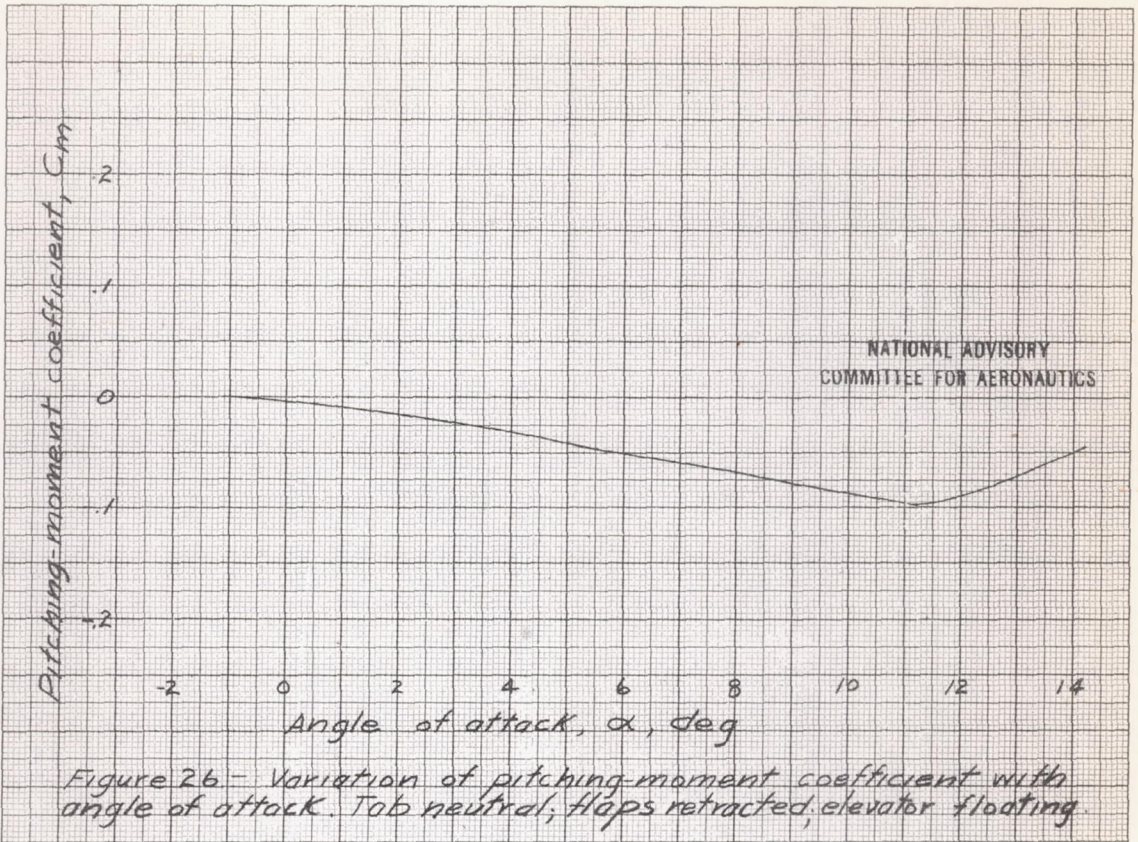


Figure 23.- Variation of elevator hinge-moment coefficient with elevator deflection at various angles of attack. Tab neutral; flaps deflected 45°.





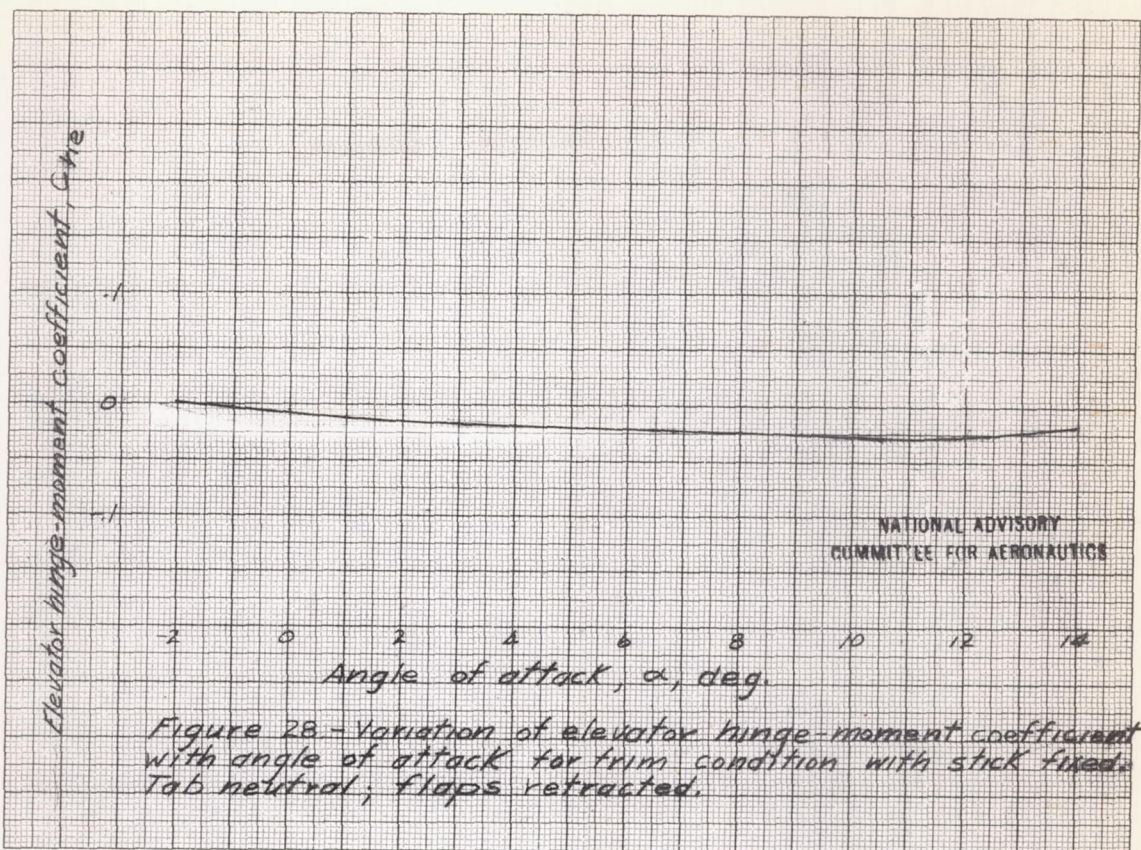


Figure 28 - Variation of elevator hinge-moment coefficient with angle of attack for trim condition with stick fixed. Tab neutral; flaps retracted.

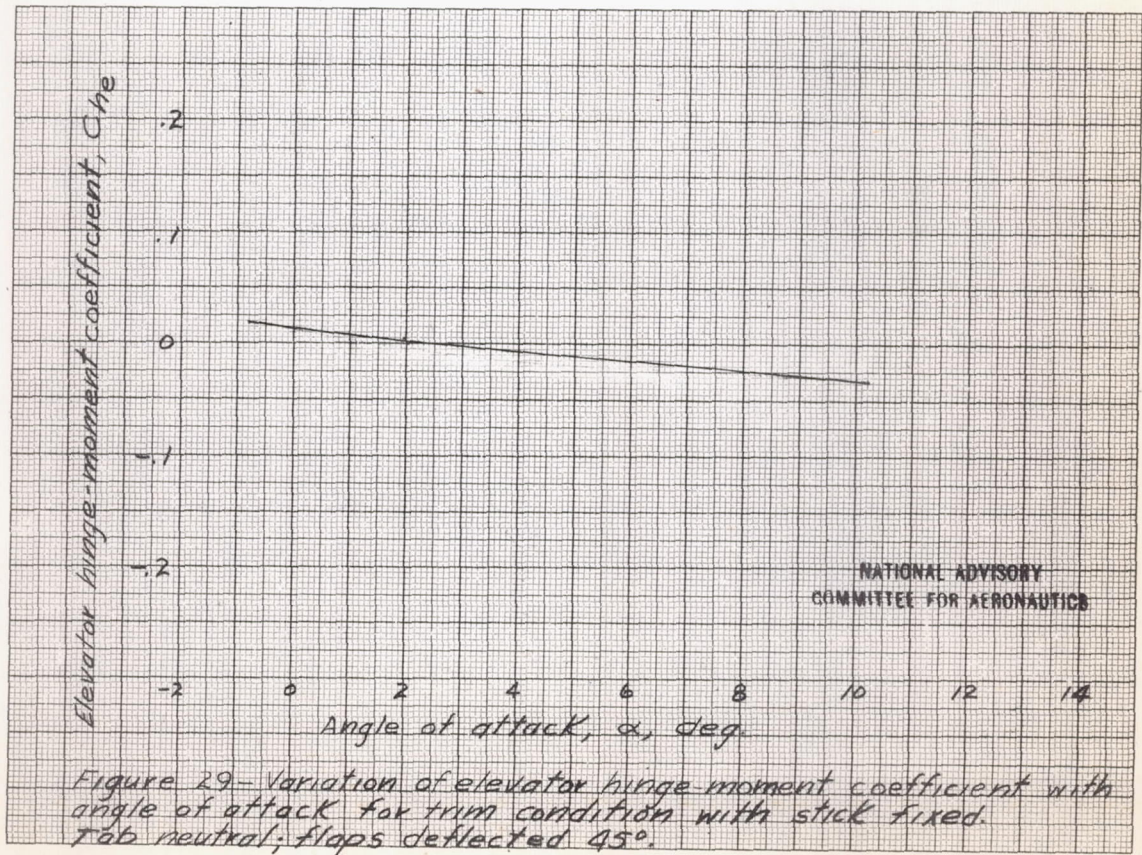


Figure 29 - Variation of elevator hinge-moment coefficient with angle of attack for trim condition with stick fixed. Tab neutral; flaps deflected 45°.

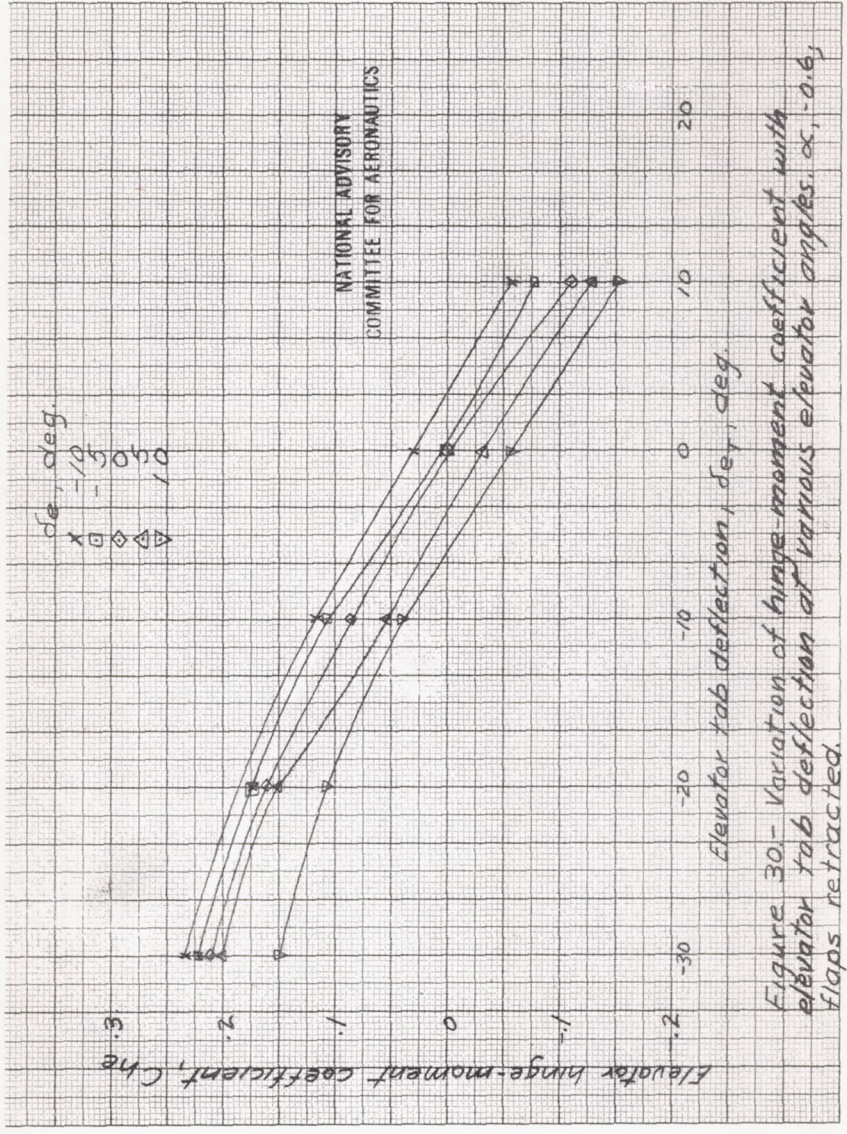


Figure 30.- Variation of hinge-moment coefficient with elevator tab deflection at various elevator angles. α , -0.6, flaps retracted.

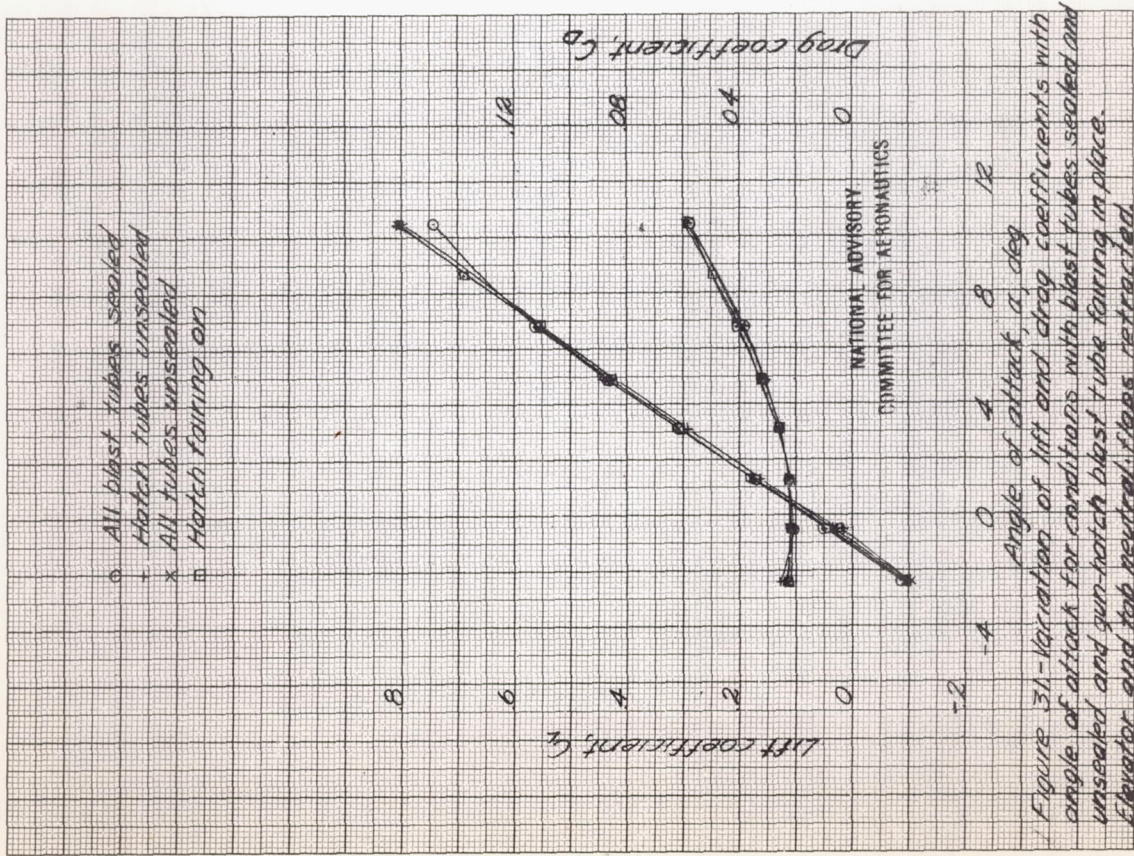


Figure 31-Variation of lift and drag coefficients with angle of attack for conditions with blast tubes sealed and unsealed and gun-hatch blast tube fairing in place. Elevator and tail neutral, flaps retracted.

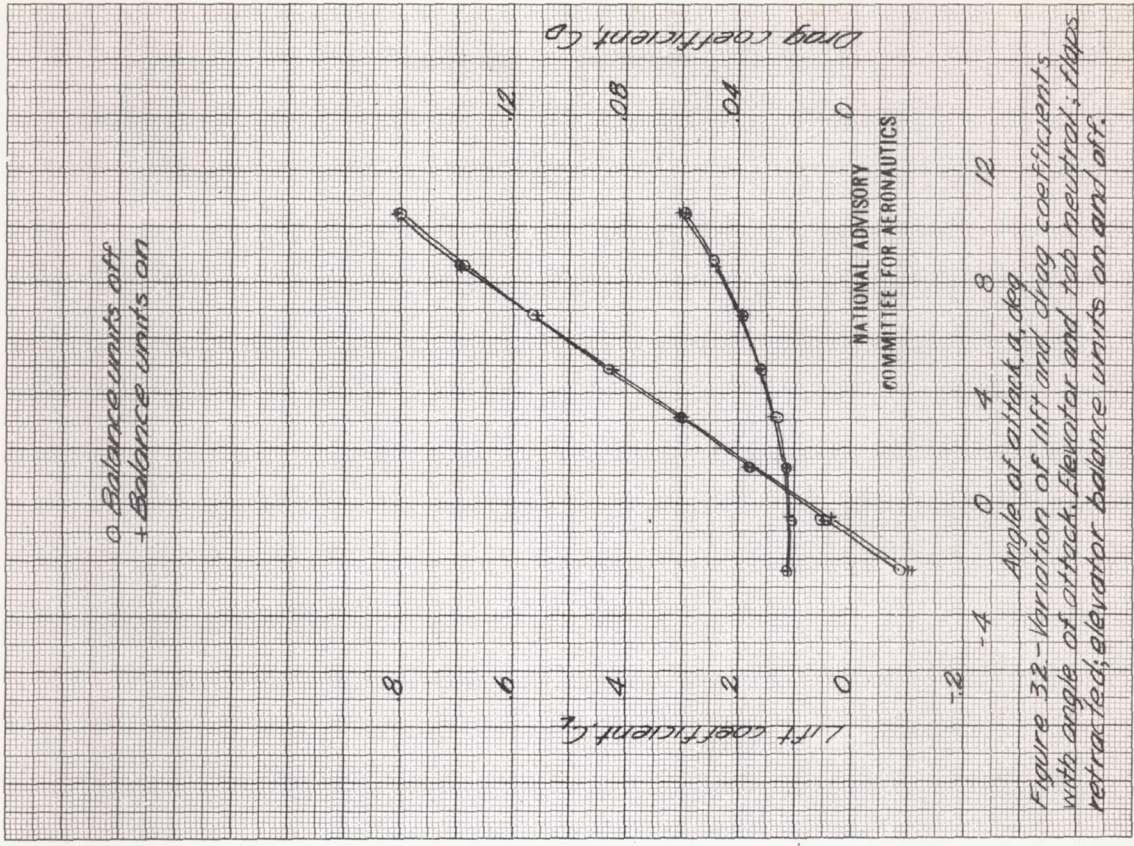
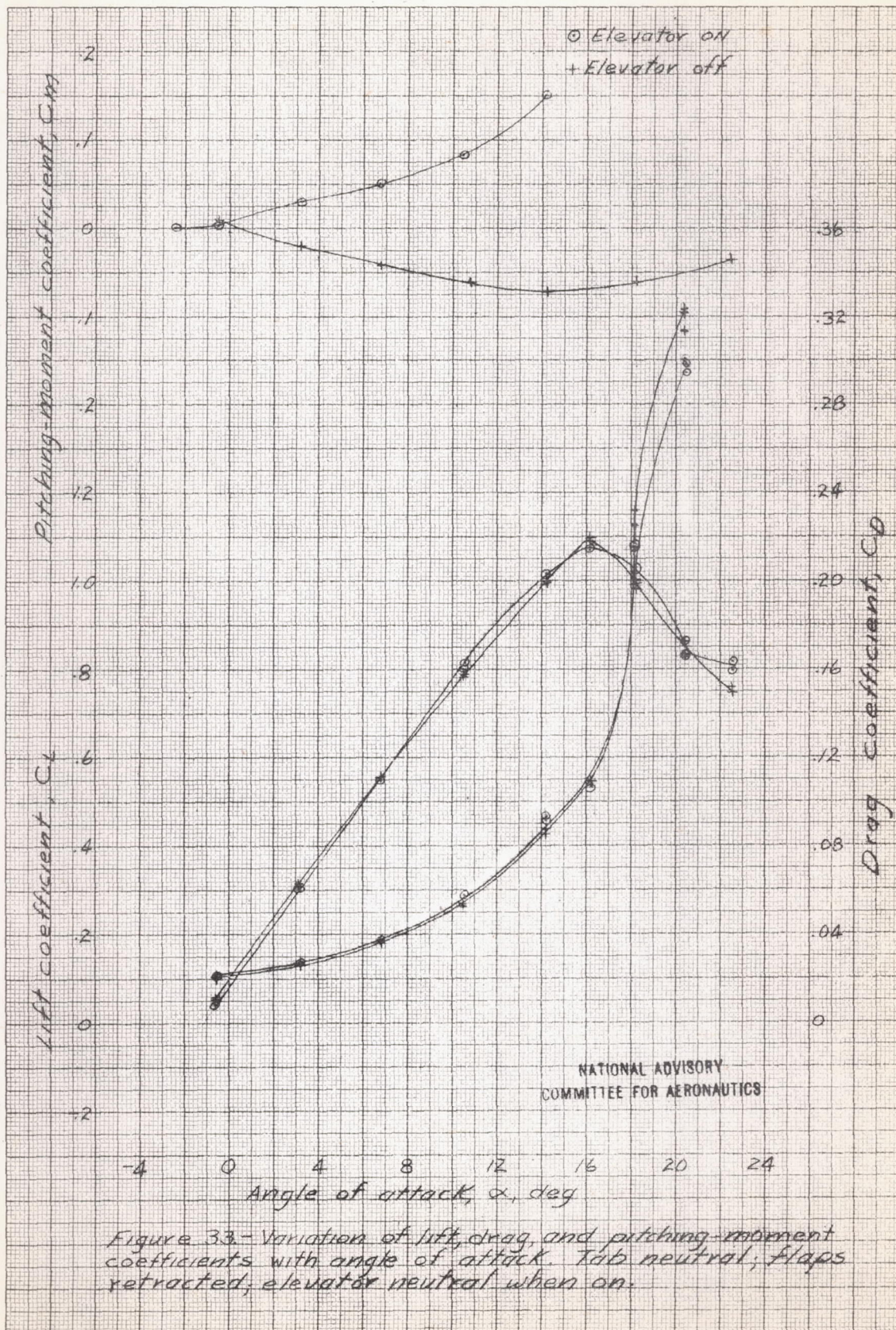
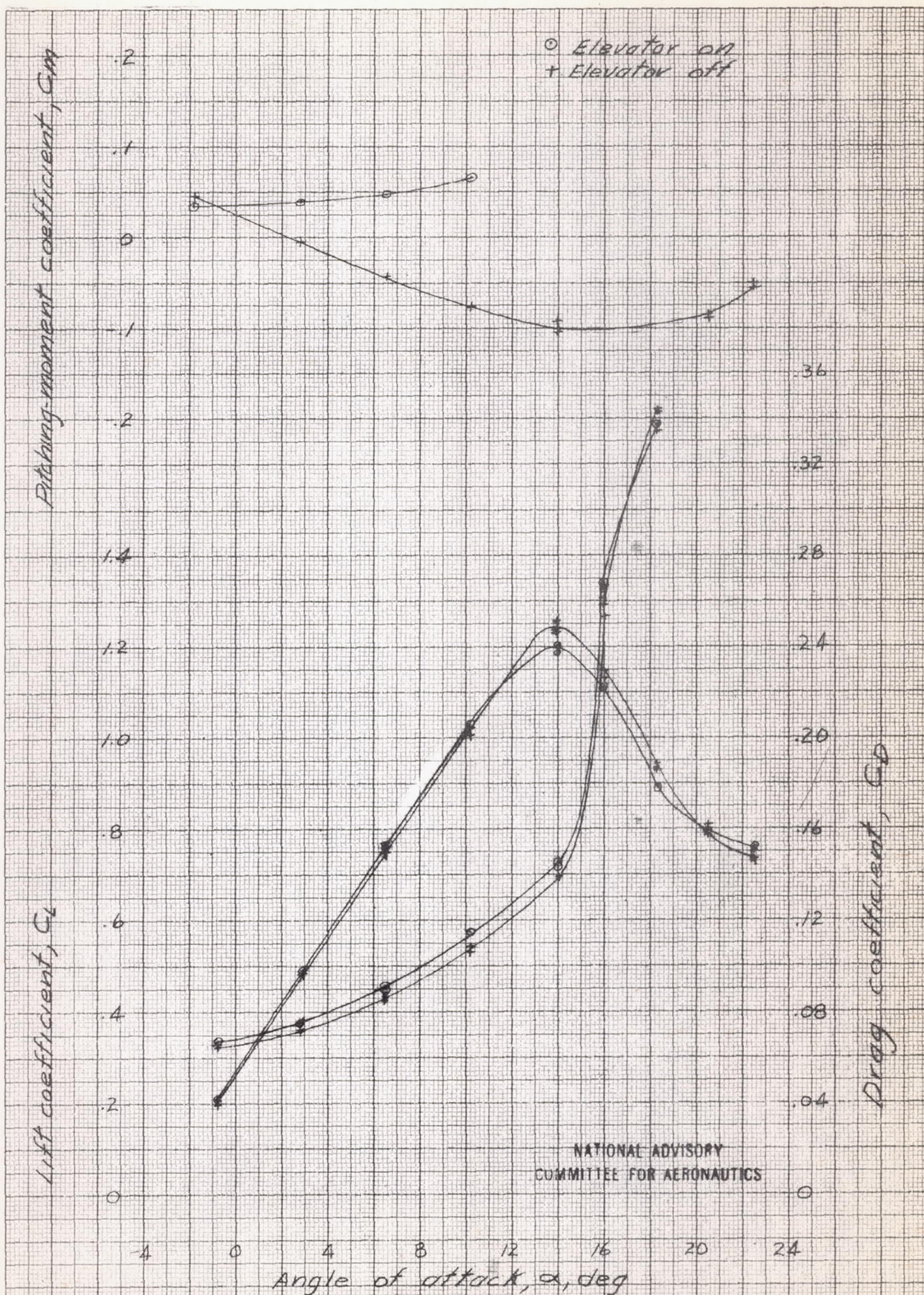


Figure 32-Variation of lift and drag coefficients with angle of attack. Elevator and tail neutral; flaps retracted; elevator balance units on and off.





NATIONAL ADVISORY
COMMITTEE FOR AERONAUTICS

Figure 34 - Variation of lift, drag, and pitching-moment coefficients with angle of attack. Tab neutral, flaps deflected 45°, elevator neutral when on.

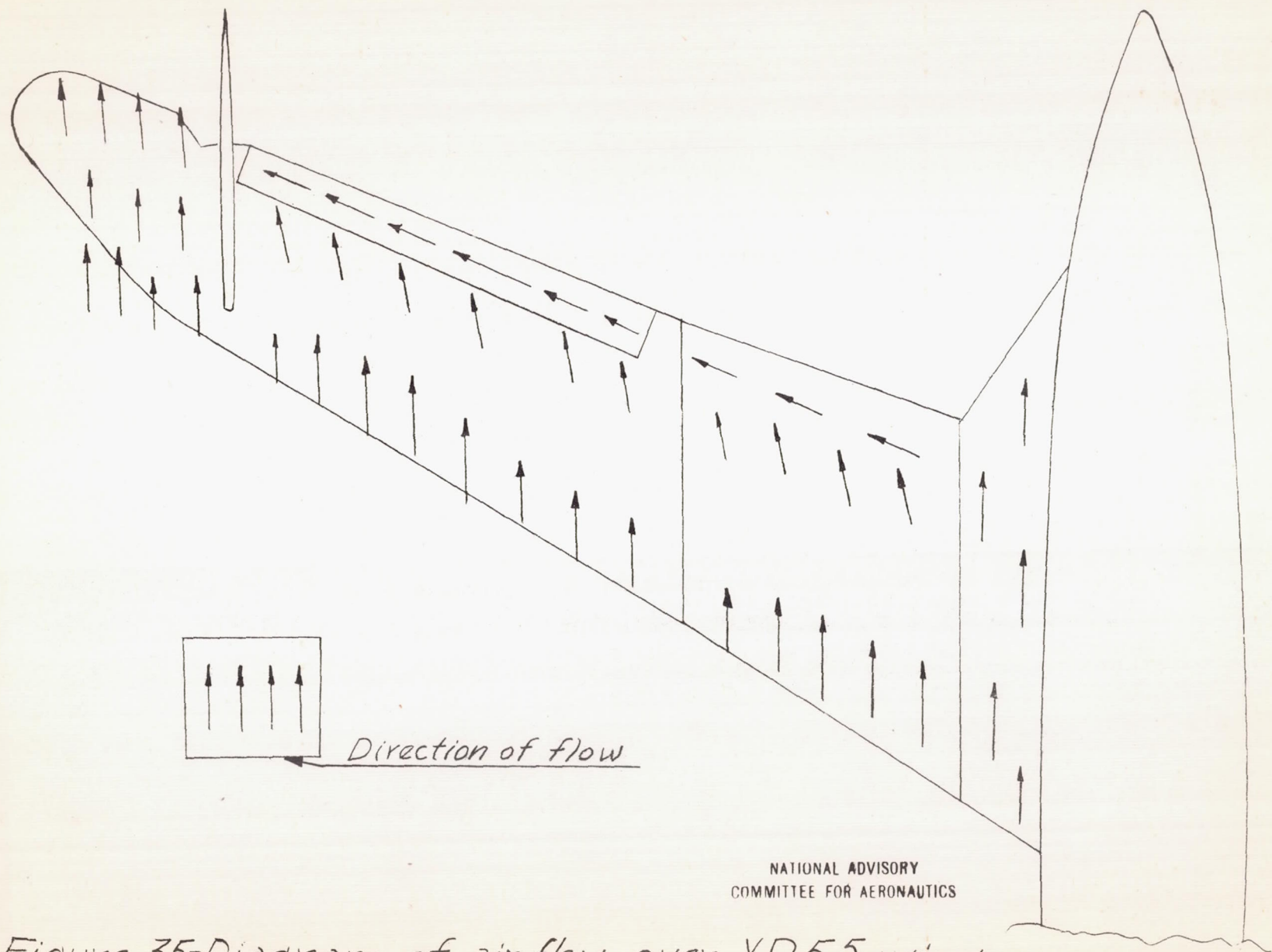


Figure 35-Diagram of air flow over XP-55 wing.
Angle of attack, 8.5° .

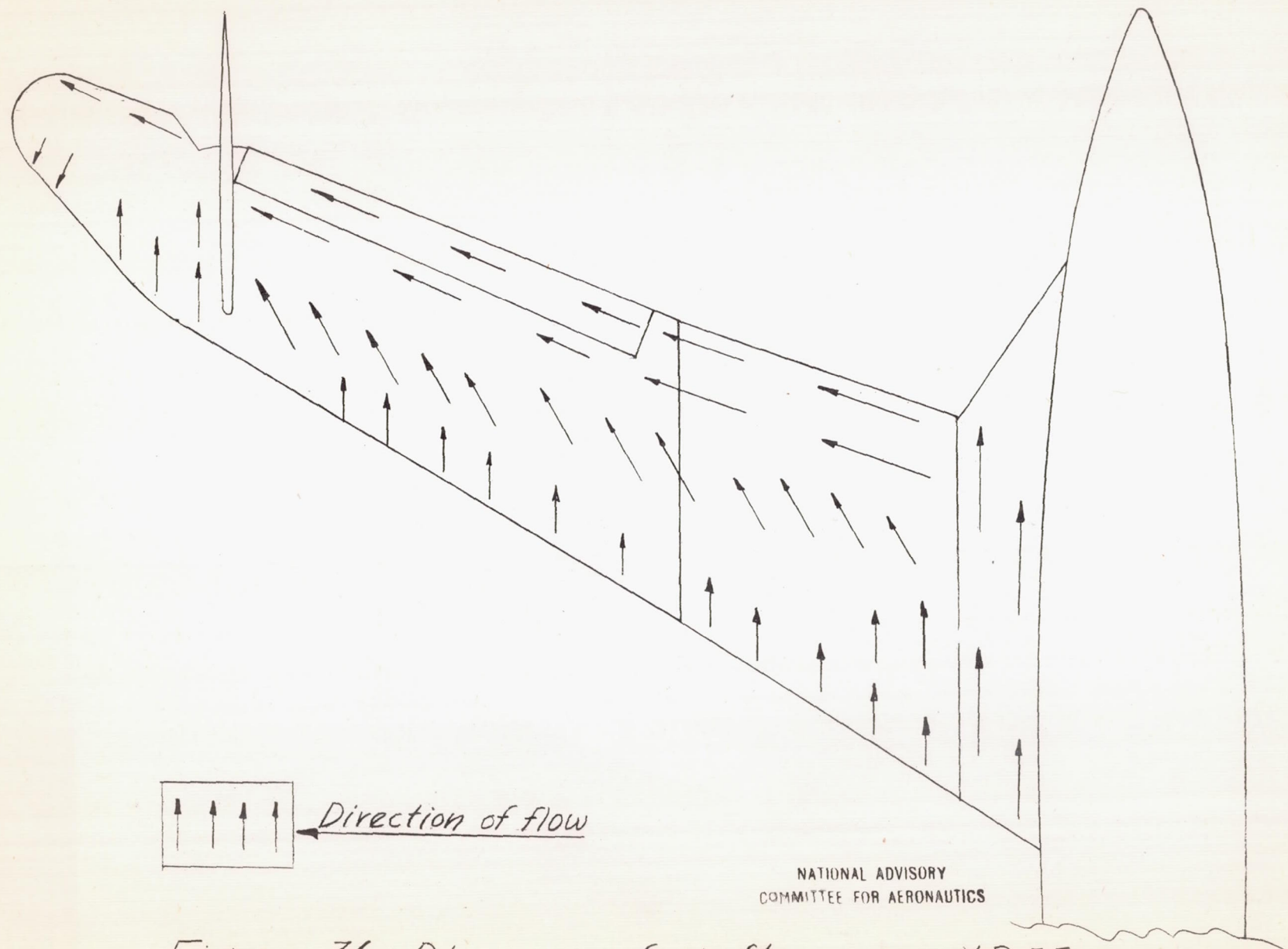


Figure 36.-Diagram of air flow over XP-55 wing. Angle of attack, 13.2°.

NATIONAL ADVISORY
COMMITTEE FOR AERONAUTICS

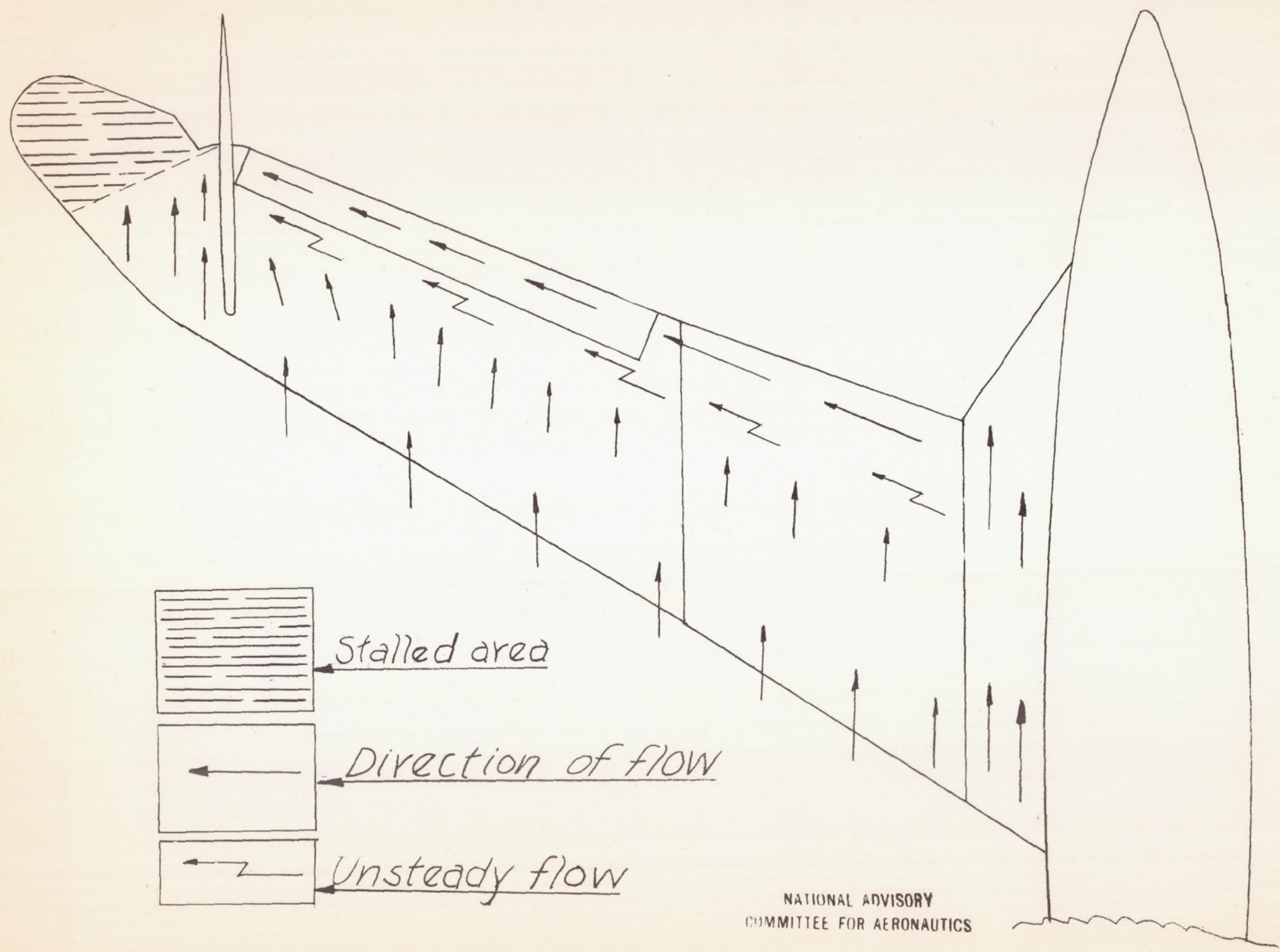


Figure 37. - Diagram of air flow over XP-55 wing.
Angle of attack, 15.1°

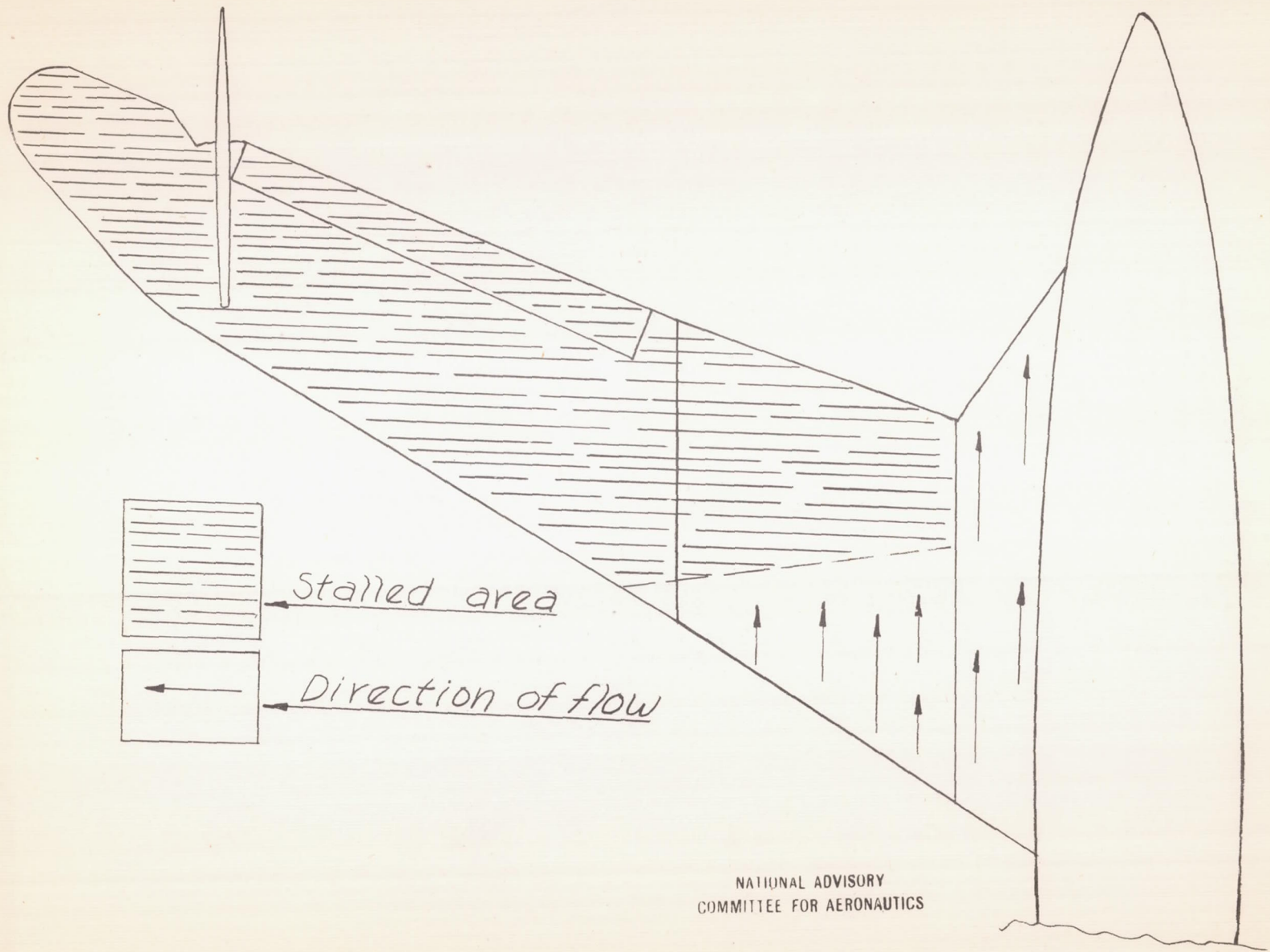


Figure 38.-Diagram of air flow over XP-55 wing. Angle of attack, 17.3°

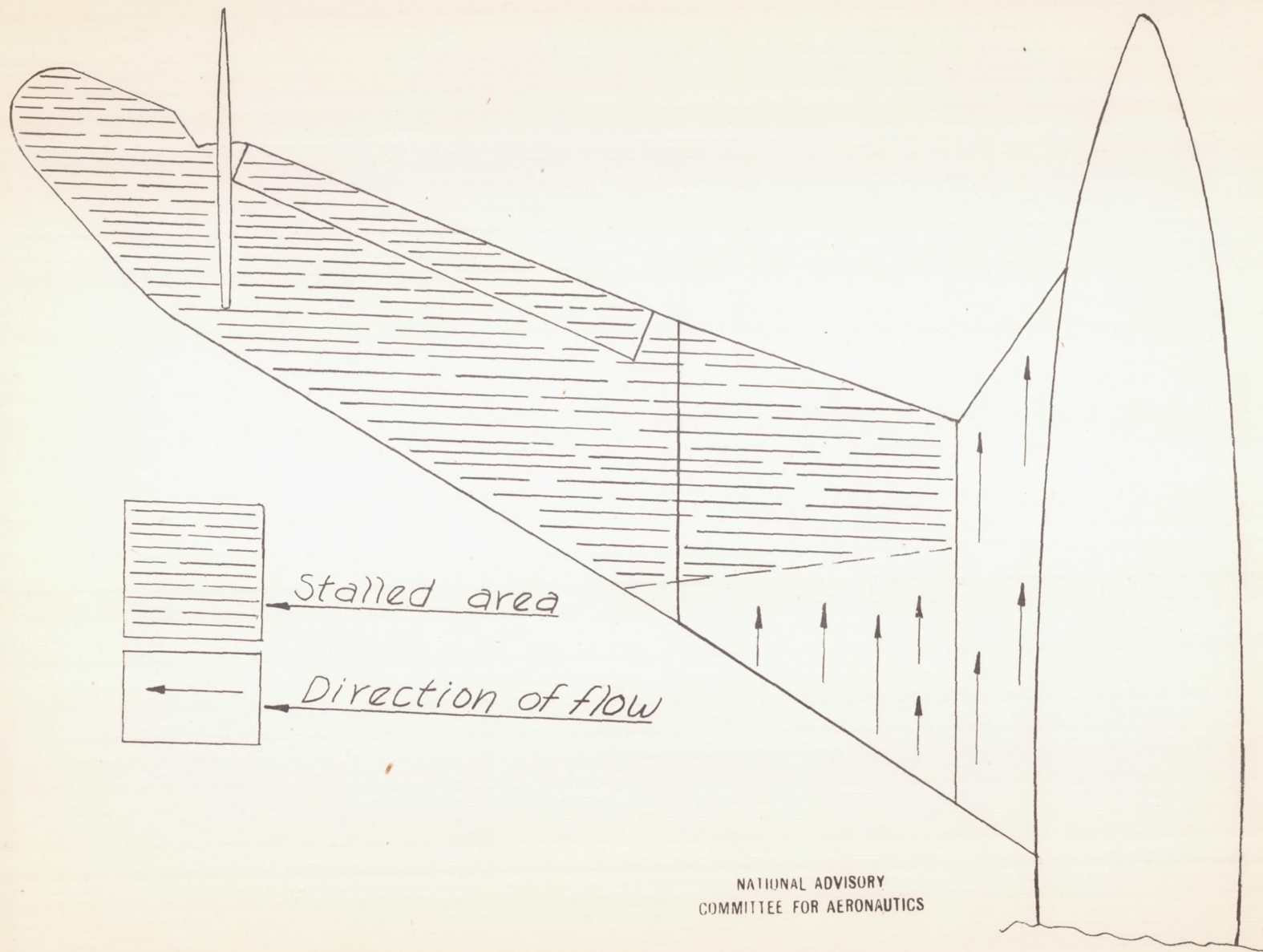


Figure 38.-Diagram of air flow over XP-55 wing. Angle of attack, 17.3°

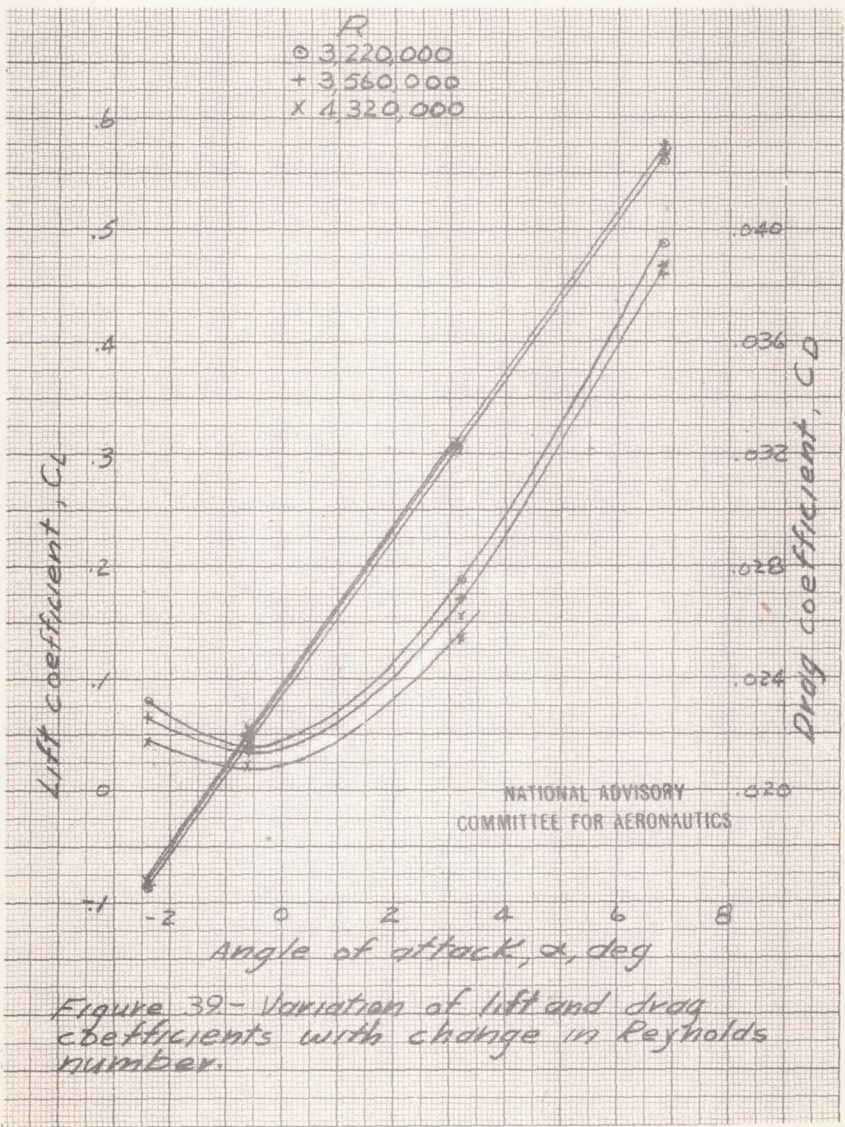


Figure 39 - Variation of lift and drag coefficients with change in Reynolds number.